NACA

RESEARCH MEMORANDU

INVESTIGATION OF EFFECTIVE THERMAL CONDUCTIVITIES OF POWDERS

By R. G. Deissler and C. S. Eian

Lewis Flight Propulsion Laboratory
Cleveland, Ohio

NATIONAL ADVISORY COMMITTEE
FOR AERONAUTICS
WASHINGTON

June 24, 1952

NATIONAL ADVISORY COMMITTEE FOR AERONAUTICS

RESEARCH MEMORANDUM

INVESTIGATION OF EFFECTIVE THERMAL CONDUCTIVITIES OF POWDERS

By R. G. Deissler and C. S. Eian

SUMMARY

A simplified analysis was made to determine the effective thermal conductivity of a powder from the fraction of space occupied by the gas and the conductivities of the solid and the gas which make up the powder. In order to check the analysis and to obtain data of current technical interest, tests were conducted to determine the conductivity of magnesium oxide powder in various gases at temperatures between 200° and 800° F. A few runs were made to determine the effect of gas pressure on thermal conductivity. Good agreement was obtained between analytical and experimental results. The effects of some of the factors neglected in the simplified analysis, such as bending of the heat-flow lines and the irregularity of the arrangement of the particles, were investigated and discussed.

INTRODUCTION

A great deal of experimental work has been done for determining the thermal conductivities of powders. A summary of experimental results is given in reference 1. Very little analytical work has been done to predict the effective thermal conductivity of a powder from the properties of the solid and gas which make up the powder. A semiempirical analysis given in reference 2 agrees with experimental data when a correction factor given in reference 1 is applied. The analysis given in the present investigation, although simplified, appears to be an improvement over existing analyses inasmuch as no correction factors are necessary.

In order to check the analysis and to obtain data of current technical interest, tests were conducted at the NACA Lewis laboratory to determine the thermal conductivity of magnesium oxide powder in various gases.

The test section was filled with magnesium oxide by the General Electric Company.

SYMBOLS

The following symbols are used in this report:

A	heat-transfer area (sq ft)
A_r	cross-sectional area of rod used in relaxation method (sq ft)
a	fraction of space in powder occupied by gas
C	constant
C'	constant
d	displacement in a given direction required to bring center of inner tube into line with center of outer tube (ft)
f	fraction of particles retained on given sieve size and passing through next larger size
Kn	Knudsen number
k	effective thermal conductivity of powder ((Btu)(ft)/(hr)(sq ft)($^{\circ}$F))
k_B	Boltzman constant (ft-lb/$^{\circ}$R)
k_g	thermal conductivity of gas ((Btu)(ft)/(hr)(sq ft)($^{\circ}$F))
k_m	average thermal conductivity, evaluated at $(t_1+t)/2$, ((Btu)(ft)/(hr)(sq ft)($^{\circ}$F))
k_{rg}	thermal conductivity of rod in gas ((Btu)(ft)/(hr)(sq ft)($^{\circ}$F))
k_{rs}	thermal conductivity of rod in solid ((Btu)(ft)/(hr)(sq ft)($^{\circ}$F))
k_s	thermal conductivity of solid ((Btu)(ft)/(hr)(sq ft)($^{\circ}$F))
k_1	thermal conductivity at r_1 ((Btu)(ft)/(hr)(sq ft)($^{\circ}$F))
L	length of tube (ft)
l_S	weighted mean sieve size required to retain particles as calculated from equation (7) (ft)
n	line number in table in Procedure, used in equation (7)
p	pressure (lb/sq ft absolute)

p_b breakaway pressure, pressure at which effective conductivity begins to vary appreciably with pressure, (lb/sq ft absolute)

Q heat transfer (Btu/sec)

R residual at a point ($^{\circ}F$)

r radius, distance from center of outer tube (ft)

r_1 reference radius where thermal conductivity is calculated, radius of outer tube (ft)

r_2 radius of inner tube (ft)

r' corrected radial location of thermocouple (ft)

r_2' $r_2 + d$ (ft)

S sieve size (ft)

s molecular diameter determined from viscosity (ft)

t temperature ($^{\circ}R$)

t_1 temperature at r_1 ($^{\circ}R$)

t_2 temperature at r_2 ($^{\circ}R$)

x coordinate (ft)

y coordinate (ft)

α temperature coefficient of thermal conductivity ((Btu)(ft)/(hr)(sq ft)$(^{\circ}F)^2$)

δ distance between intersections of rods (ft)

θ angle

λ mean free path of gas molecules (ft)

ANALYSIS

An exact theoretical determination of the effective thermal conductivity of a powder from the properties of the solid and the gas which make up the powder could probably not be made at present because the particles in most powders are irregularly arranged and may be of various shapes and sizes. It is therefore expedient to use approximate methods and to check the results by experiment.

Maximum and Minimum Limits of Thermal Conductivity of a Two-Phase System

Before the analysis of a powder is made, it is of value to obtain the maximum and minimum limits of the thermal conductivity of any two-phase system. The maximum thermal conductivity of a two-phase system, such as a solid-gas system, is attained when the materials are arranged in alternate layers separated by planes parallel to the direction of heat flow. The minimum conductivity of such a system is attained when the materials are separated by planes perpendicular to the direction of heat flow. These two cases are shown in figure 1, where the ratio of the conductivity of the solid k_s to the conductivity of the gas k_g is plotted against the ratio of the effective conductivity of the system k to the conductivity of the gas for various fractions a of space occupied by the gas. For $a = 0.4$ and $k_s/k_g = 2$, there is a possible variation of the effective conductivity from the average of about ±7 percent, whereas for $k_s/k_g = 1,000$ there is a possible variation of ±99 percent. This indicates that the effective conductivity of a system for a given fraction of space occupied by the gas is greatly influenced by the arrangement of material for high values of k_s/k_g, whereas for low values of k_s/k_g the arrangement of material is of lesser importance. Inasmuch as k_s/k_g is high for most powders, the arrangement of material must be accounted for in an analysis of conductivities of powders.

Simplified Analysis for Powders

The most important characteristic of powders, insofar as it affects their thermal conductivities, is the presence of small regions or points of contact between the particles of solid in the powder. For high values of k_s/k_g most of the heat flow takes place in the vicinity of these points because the gas acts as an insulator at points where the particles are separated.

In the present analysis the particles are assumed to be spheres or cylinders arranged in cubical or square array with point or line contacts. It is also assumed that the heat flow is in the same direction at every point; that is, the bending of the heat-flow lines is neglected. Irregularity in the arrangement of the particles would produce a decrease in heat flow, whereas bending of the heat-flow lines would produce an increase, so that the two effects tend to cancel each other. The effect of the bending of the heat-flow lines on the heat transfer will be investigated in Refined Analysis.

For solid spheres in cubical array in a gas as shown in figure 2(a), k/k_g is found in appendix A to be given by

$$\frac{k}{k_g} = \frac{1}{2}\frac{\pi}{\left(\frac{k_g}{k_s} - 1\right)^2}\left[\left(\frac{k_g}{k_s} - 1\right) - \log_e \frac{k_g}{k_s}\right] + 1 - \frac{\pi}{4} \tag{1}$$

For spheres in cubical array, the fraction of space occupied by the gas is 0.475.

For solid cylinders in square array in a gas, k/k_g is found in appendix A to be given by

$$\frac{k}{k_g} = \frac{\pi}{2\left(\frac{k_g}{k_s} - 1\right)} - \frac{\frac{\pi}{2} - \sin^{-1}\left(\frac{k_g}{k_s} - 1\right)}{\left(\frac{k_g}{k_s} - 1\right)\sqrt{2\frac{k_g}{k_s} - \left(\frac{k_g}{k_s}\right)^2}} \tag{2}$$

For cylinders arranged in square array, a = 0.214.

The values of k/k_g for $a = 0$ and $a = 1$ are also known. For $a = 1$, $k/k_g = 1$; for $a = 0$, $k/k_g = k_s/k_g$. The relation between k/k_g and k_s/k_g is therefore known for four values of a so that the relation for any value of a can be determined with fair accuracy by interpolation for a given value of k_s/k_g. In this way the thermal conductivity of a powder can be estimated if the conductivity of the solid, the conductivity of the gas, and the fraction of space occupied by the gas are known.

Refined Analysis

In order to determine the effect of bending of the heat-flow lines on the heat transfer through a powder, the heat flow through solid cylinders in a gas was calculated exactly for several arrangements of cylinders by the method of relaxation. The application of the relaxation method to heat-conduction problems in single-phase systems is described elsewhere. In appendix B the method is applied to the calculation of heat conduction in two-phase systems. Calculations are carried out for cylinders in square array with the heat flow as shown in figure 2(a), for cylinders in square array with the heat flow at 45° to the direction shown in figure 2(a), and for cylinders in triangular array as shown in figure 2(d). For each case k/k_g is obtained as a function of k_s/k_g.

The refined analysis may not predict the thermal conductivity of a powder more closely than the simplified analysis because it still does not account for irregularity of arrangement of particles.

EXPERIMENTAL INVESTIGATION

Apparatus

The apparatus used in this investigation is described in the following sections.

Test section and gas chamber. - A drawing of the test section enclosed in a gas chamber and cooling jacket is shown in figure 3(a). The test section consists essentially of a wound-wire-type heating element with individual end-guard heater elements centrally enclosed in a monel tube containing the powder under investigation. Thermocouples are stretched longitudinally through the tube to obtain the radial temperature distribution through the powder.

The heating elements are number 16 Nichrome wire wound on an 18-inch length of 3/8-inch-outside-diameter high-temperature porcelain tube. The main heater is 14 inches long and the end-guard heaters are each $1\frac{5}{8}$ inches long. The heater leads pass through holes ground radially through the tube walls and thence out the open ends of the tube where copper wire is joined to the leads for transmitting electric power to the heater elements. All the Nichrome coils are coated with a high-temperature ceramic cement to give a smooth outer surface.

Temperatures are measured not only near the inner and outer surfaces of the tube containing the powder under investigation, but also at several radial locations through the powder. This method of temperature measurement was selected because of the difficulty in accurately measuring surface temperatures, especially that of the ceramic-coated heater element, and also to avoid measurements which might include contact resistance between the powder and container surfaces. These temperatures are obtained at 1/8-inch intervals by stretching number 28 chromel-alumel thermocouple wires through holes drilled in ceramic disks which are fitted to each end of the porcelain tube. Four groups (90° apart) of five radially positioned thermocouple wire junctions are located in a plane across the center of the test section. Two of these groups are shown in figure 3(a). The ceramic disks also serve as end plugs to contain the powder. Mica spacers located 1 inch from either side of the thermocouple junctions aid in maintaining the distance between thermocouples while filling the test section with the powder. The thermal conductivity of mica is of the same order of magnitude as that of the powder. Temperatures are also measured near the surface at the center and ends of the main heater element by imbedding thermocouples on the ceramic coating of the heater coils.

The heater-element and thermocouple-wire assembly is inserted into a monel tube having a length of 18 inches, an inside diameter of $1\frac{3}{4}$ inches, and an outside diameter of 2 inches, and is held in place by set screws in contact with the ceramic disks at each end of the tube. The outside-surface temperature of the monel tube is measured at the center and end positions of the main heater element by two chromel-alumel thermocouples located 180° apart at each position.

A porous, stainless-steel disk welded into a hole in the outer monel tube wall allows gas passage into and out of the powder voids.

The test section is centrally located in a gas chamber consisting of a 22-inch length of 6-inch standard pipe and is supported by two ceramic knife edges to minimize local heat conduction from the monel tube. The 6-inch pipe, in turn, is enclosed in a length of 8-inch standard pipe. The two pipes are joined by annular flanges to form an annular passage through which cooling water is circulated. At each end of the test section, the heater element and the thermocouple leads are brought out of the gas chamber between two $\frac{1}{8}$-inch neoprene gaskets and, with a $\frac{3}{4}$-inch-thick flange and $12\frac{1}{2}$-inch bolts, form an effective gas seal. Silicon-type high-vacuum grease applied to the neoprene gaskets aids in preventing leakage at low pressures within the gas chamber and test section.

Associated equipment. - A schematic diagram of the test section and associated apparatus is shown in figure 3(b). By means of suitable tube connections to a hole drilled in each flange of the gas chamber, the test section may be evacuated by the use of a vacuum pump at the outlet end or supplied with laboratory high-pressure air, bottled helium, or argon gases at the inlet end. An indicating-type anhydrous calcium sulphate desiccant is incorporated in the air supply line, while the helium and argon gases used are "grade A" commerically purified and bottled. Gas chamber pressure is measured by a calibrated aircraft-type manifold pressure gage.

The 110-volt, 60-cycle power is individually supplied to the main heater and each guard heater and is individually controlled by variable transformers of 2 kilovolt-ampere capacity. Copper leads are attached by clips to the Nichrome heater leads as close as possible to the ends of the test section. Power to the main heater is measured by a calibrated ammeter, voltmeter, and wattmeter.

Temperature readings are obtained by a self-balancing indicating-type potentiometer.

Procedure

The test section was filled through a hole provided in one of the ceramic end disks with granular magnesium oxide M_gO giving a fractional volume occupied by the solid particles of 0.58. The filling was done on a vibratory table. The particle size of the M_gO used in the investigation as given by the manufacturer is given in table I.

The distances between the junction of the thermocouple wires stretched through the powder and their positions relative to the outside container wall and main heating element were obtained from X-ray photographs taken of the test section after it was filled. Negatives of the photographs were then inserted into an enlarging-type film viewer from which the measurements were obtained at a X12 magnification, thus enabling a high degree of accuracy to be attained. As a result of damage during shipment, two of the four groups of thermocouples in the powder were indicated by the photographs to be so disarranged as not to warrent their use, and therefore the calculation of the data was based on the remaining two groups.

Data were obtained for air, helium, and argon gases over a range of average powder temperatures of 200° to 800° F and pressures of 0.15 to 110 pounds per square inch absolute. Replacement of one gas by another in the powder was accomplished by purging the entire system with the vacuum pump several times, letting the gas to be used flow in before each evacuation. The desired gas pressure was held constant during each run. A small rate of water flow through the outer cooling jacket was maintained constant throughout each run.

The power input to the main heater element was adjusted for each run to give the desired temperature. The power input to each of the end-guard heaters was then adjusted to maintain a uniform temperature over the main heater element in order to prevent axial heat flow.

After equilibrium conditions had been reached, the following quantities were measured: power input to the main heating section, temperatures of the heating elements, temperatures through the powder, outside surface temperatures of the monel tube, and gas pressure.

For some of the runs, check points were taken after additional purging of the test section; in each case good agreement of the data with that of the initial run was obtained.

Reduction of Experimental Data

Equation for heat flow through concentric cylinders. - The equation for the heat flow through two concentric cylinders with uniform surface temperatures and a temperature-dependent thermal conductivity between the cylinders is

$$Q = \frac{2\pi k_m L(t_1 - t)}{\log_e\left(\frac{r}{r_1}\right)} \tag{3}$$

where t_1 and t are temperatures at the radii r_1 and r, and k_m is evaluated at $(t_1+t)/2$. The derivation of equation (3) and the conditions under which k_m can be evaluated at $(t_1+t)/2$ are given in appendix C.

Calculation of thermal conductivity. - In calculating the thermal conductivity of the powder from the temperatures measured at various radii and the heat flow, it is desirable to plot the temperature against such a quantity that the plot is a straight line. This can be done by rewriting equation (3) as follows:

$$t = t_1 - \frac{Q}{2\pi k_1 L}\left[\frac{k_1}{k_m}\log_e\left(\frac{r}{r_1}\right)\right] \tag{4}$$

where t_1 and k_1 are evaluated at the fixed reference radius r_1. Equation (4) shows that, if t is plotted against $(k_1/k_m)\log_e(r/r_1)$, the plot will be a straight line with slope $-Q/(2\pi k_1 L)$. The thermal conductivity k_1 at temperature t_1 can be calculated from

$$k_1 = -\frac{Q}{2\pi L}\frac{1}{\text{slope}} \tag{5}$$

For plotting equation (4), a relation between k and t must be assumed in order to calculate k_1/k_m. After equation (4) is plotted, the conductivity is calculated from equation (5). If the assumed values of k differ greatly from those calculated from equation (5), the calculations are repeated using the new values.

By the use of the preceding method, a large number of thermocouple readings is used for determining each value of conductivity so that errors in conductivity caused by errors in temperature measurements are small. A typical temperature plot is shown in figure 4.

Correction for eccentricity of tubes. - It was found from the X-ray photographs of the test section that the center of the inner tube was displaced about 0.02 inch from the center of the outer tube at the cross section where the radial temperature measurements were made. In order to locate the thermocouples at the positions they would occupy if the tubes were concentric, a correction derived in appendix D was applied to the measured locations of the thermocouples.

Thermal conductivities of gases and solid magnesium oxide. - In order to compare the analytical and experimental results, it is necessary to use values for the thermal conductivities of solid magnesium oxide and of the various gases used in the tests. For solid magnesium oxide, the approximate values given in reference 3 were used. These values are plotted in figure 5. The values of k for argon and helium were calculated from the kinetic theory relation $k = 2.5\mu c_v$, where the viscosity μ was obtained from reference 4 and the values of c_v were found from the kinetic theory to be 0.745 (Btu/(lb)(°F)) for helium and 0.0747 (Btu/(lb)(°F)) for argon. The kinetic theory relation for thermal conductivity was used in preference to experimental values of k because experimental values of viscosity are, in general, more reliable than those of conductivity and because the kinetic theory relation is generally considered accurate for monatomic gases. The conductivities of helium and argon are plotted in figures 6(a) and 6(b), respectively. For air the thermal conductivity was obtained from reference 5 and is plotted in figure 6(b).

RESULTS AND DISCUSSION

Predicted Effective Thermal Conductivities

Predicted curves for determining the effective thermal conductivity of a powder from the simplified analysis are shown in figures 7 and 8. The effective thermal conductivity of a powder can be obtained from these curves when the thermal conductivities of the solid and the gas and the fraction of space occupied by the gas are known. The curves indicate that the effective conductivity increases at an increasing rate as the fraction of space occupied by the gas decreases.

Experimental Effective Conductivities

Experimental thermal conductivities of magnesium oxide powder in air, helium, and argon for temperatures between 200° and 800° F are plotted in figure 9. The conductivity of the powder increases with temperature for each gas. This indicates that a change in the conductivity of the gas is more important than a change in the conductivity of the solid in determining a change in the conductivity of the powder, inasmuch as the conductivity of the solid decreases with temperature. The conductivity of the powder in helium is much greater than in the other gases because of the much greater conductivity of helium.

Comparison of Analytical and Experimental Results

A comparison of the analytical results with the experimental results from the present investigation is given in figure 10(a). The agreement is good, especially at low temperatures. At high temperatures the deviation, a maximum of 20 percent, may be caused by errors in the conductivities used for the constituents of the powder or by factors neglected in the analysis.

A comparison of the analytical results from the simplified analysis with representative experimental results of other investigators from reference 1 is given in figure 10(b). The powders tested included six different solid materials and values of a from 0.24 to 0.518. It is seen from the figure that the agreement between analytical and experimental results in most cases is very good.

Refined Analysis

A comparison of the simplified analysis with exact or relaxation solutions for regularly arranged cylinders and squares is given in figure 11. The values for squares (arranged in checkerboard fashion, a = 0.5) are from reference 6, where it is shown that $k/k_g = \sqrt{k_s/k_g}$ for heat flow in any direction parallel to the plane of the squares. The exact solutions give substantially higher values for effective conductivity than does the simplified analysis. The agreement of the experimental data with the simplified analysis where the bending of the heat-flow lines is neglected is, however, much better than the agreement with the refined analysis where the bending of the lines is considered. It is concluded that a factor is neglected in the simplified analysis which compensates for the effect of bending of the heat-flow lines.

In most powders the particles are irregularly arranged and may be of irregular shape and size. However, the data in figure 10, which agree closely with the simplified analysis, include steel and lead balls of uniform diameter as well as particles of irregular shape and size so that the shape and the size of the particles do not seem to be pertinent factors in determining the conductivity. The good agreement of the simplified analysis and the poor agreement of the refined analysis with experiment seem to be caused by the irregular arrangement of the particles. For a given fraction of space occupied by the gas, the particles, when in irregular arrangement, may be closer together at some points and farther apart at other points than when in regular arrangement. For example, if cylinders in square array are arranged in triangular array with the same fraction of gas space as in square array, the cylinders are in contact on one side only and the effective thermal conductivity of the system is greatly reduced. In powders where the particles are irregularly arranged, it appears that some of the particles are in contact on one side only and that this produces a decrease of effective thermal conductivity. The good agreement of the simplified analysis with experimental is partially fortuitous inasmuch as there was no way of knowing that the effect of the bending of the heat-flow lines is exactly cancelled by the effect of irregularity of arrangement of particles.

Typical temperature distributions for the configurations for which the effective thermal conductivities were calculated by the relaxation method are shown in figure 12. For a temperature difference between the top and bottom surfaces of 1° F, the lines represent constant temperatures at intervals of 0.1° F. The constant temperature lines are crowded together in the vicinity of the points of contact of the particles and the crowding of the lines is increased as k_s/k_g is increased. This indicates that most of the heat flow in a powder takes place in the vicinity of the points of contact.

Effect of Pressure on Conductivity

The effect of gas pressure on the effective thermal conductivity of magnesium oxide powder is shown in figure 13. For each curve there is a range of pressures for which the thermal conductivity is constant. Below this range the conductivity decreases rapidly as the pressure is reduced to zero. The pressure range for constant conductivity varies with temperature and is different for different gases.

The observed effects of pressure can be explained by the kinetic theory of gases. For the range where the pressure has no effect on conductivity, the mean free path of the gas molecules is small compared with the distances between the particles which are effective in transferring heat. For the long mean free paths which are obtained at low pressures or high temperatures the conductivity varies with pressure. The mean free path of the gas molecules also depends on the diameter of the molecules. The kinetic theory expression for the mean free path is

$$\lambda = \frac{k_B t}{\pi \sqrt{2} p s^2} \tag{6}$$

From dimensional analysis the ratio of mean free path to a characteristic dimension of the gas spaces (Knudsen number) must have a value, independent of the gas, the temperature, or the pressure, at which the conductivity begins to vary appreciably. Inasmuch as the size of the gas spaces is of the same order of magnitude as the size of the particles, the characteristic dimension is taken as the weighted mean size of sieve required to retain the particles. It is calculated from the data given in table I by the following equation:

$$l_S = \sum_{n=1}^{7} \left(\frac{S_n + S_{n+1}}{2} \right) f_{n+1} + S_9 f_9 \tag{7}$$

and is found to be 0.00067 feet. The subscript 9 refers to the line number in the table. The Knudsen number is given by

$$Kn = \frac{\lambda}{l_S} = \frac{k_B t}{\pi \sqrt{2} p s^2 l_S} \tag{8}$$

From the data for air, the pressure at which the conductivity begins to vary with pressure (breakaway pressure) is about 15 pounds per square inch at 340° F. The molecular diameter s for air is about 9.9×10^{-10} feet so that the breakaway Knudsen number as calculated from equation (8) is about 0.00072. Inasmuch as this Knudsen number should be independent of the gas, the temperature, or the pressure, this can be used to predict the breakaway pressures for other gases. Insertion of the value 0.00072 for Knudsen number in equation (8) gives, for the breakaway pressure,

$$p_b = 1770 \times 10^{-24} \frac{t}{s^2 l_S} \tag{9}$$

For helium, $s = 6.23 \times 10^{-10}$ feet and p_b from equation (9) is 5850 pounds per square foot or about 41 pounds per square inch at 400° F. This value of breakaway pressure is in approximate agreement with the data for helium. For higher temperatures the data indicate that the breakaway pressure increases. This is also in agreement with equation (9). For argon the molecular diameter is about the same as for air so that the breakaway pressures for the two gases should be about the same, as indicated by the data. Equation (9) is therefore in approximate agreement with the data for the three gases.

Equation (9) indicates a breakaway pressure above atmospheric pressure at temperatures above 400° F for all the gases tested in the powder For the thermal conductivities plotted in figure 9, the pressures were, in all cases, above those given by equation (9).

The value of Knudsen number corresponding to the breakaway pressure is seen to be much less than unity, 0.00072. This can be explained by the fact that most of the heat transfer through a powder takes place in the immediate vicinity of the points of contact of the particles so that the dimensions effective in transferring heat in the gas spaces are much less than the dimensions of the particles.

Effect of Free Convection on Conductivity

The curves in figure 13 indicate that free convection is not an important factor in determining the effective thermal conductivity of the powder because at high pressures the thermal conductivity is independent of pressure. If there were appreciable free convection in the powder, the conductivity would continue to increase with pressure inasmuch as free convection is a function of the density of the gas.

SUMMARY OF RESULTS

The following results were obtained from the investigation of effective thermal conductivities of powders:

1. Good agreement was obtained between the effective thermal conductivities calculated from the simplified analysis and the experimental data from both the present investigation and from other investigations.

2. The agreement of exact solutions for heat flow through regularly arranged cylinders and squares with experiment was not nearly as good as the agreement of the experimental data with the simplified analysis where the bending of the heat-flow lines was neglected. The result can be explained by assuming that the particles are irregularly arranged so that some of them are in contact on one side only. The good agreement of the simplified analysis with experiment indicated that the increase in conductivity caused by bending of the heat-flow lines was cancelled by the decrease caused by irregular arrangement of particles.

3. The effective conductivity of a powder became nearly independent of pressure at some ratio of mean free path of gas molecules to a characteristic dimension of the powder particles.

Lewis Flight Propulsion Laboratory
National Advisory Committee for Aeronautics
Cleveland, Ohio

APPENDIX A

SIMPLIFIED ANALYSIS FOR HEAT FLOW THROUGH A POWDER

The particles of solid are assumed to be spheres or cylinders arranged in cubical or square array in this analysis. Bending of the heat-flow lines is neglected.

Heat Flow Through Spheres in Cubical Array

In order to obtain the effective thermal conductivity of a material made up of solid spheres in cubical array in a gas, it is necessary only to determine the heat flow through the representative sample shown in figure 2(b). The heat flow through this sample is equal to the effective thermal conductivity because unit temperature difference and unit dimensions are used. The heat flow through the infinitesimal cylindrical element of thickness dx is

$$dQ = \frac{\pi}{2} x \, dx \frac{k_s}{\sin \theta} (1 - t) \tag{1A}$$

or

$$dQ = \frac{\pi}{2} \frac{x \, dx}{1 - \sin \theta} k_g t \tag{2A}$$

where t is the temperature at the surface of the sphere. From equations (1A) and (2A), t is obtained:

$$t = \frac{1}{1 + \frac{k_g}{k_s} \frac{\sin \theta}{1 - \sin \theta}} \tag{3A}$$

Elimination of t from equations (2A) and (3A) and substitution of $x = \cos \theta$ and $dx = - \sin \theta \, d\theta$ result in

$$dQ = - \frac{\pi}{2} k_g \frac{\sin \theta \cos \theta}{1 - \sin \theta + \frac{k_g}{k_s} \sin \theta} d\theta \tag{4A}$$

The total heat flow through the sample is

$$Q = \frac{\pi}{2} k_g \int_0^{\frac{\pi}{2}} \frac{\sin\theta \cos\theta}{1 + \left(\frac{k_g}{k_s} - 1\right) \sin\theta} d\theta + \left(1 - \frac{\pi}{4}\right) k_g \tag{5A}$$

where the last term in the equation is the heat flow through the area abcd. Carrying out the integration and replacing Q by k result in

$$\frac{k}{k_g} = \frac{1}{2} \frac{\pi}{\left(\frac{k_g}{k_s} - 1\right)^2} \left[\left(\frac{k_g}{k_s} - 1\right) - \log_e \frac{k_g}{k_s}\right] + 1 - \frac{\pi}{4}$$

which is the same as equation (1).

Heat Flow Through Cylinders in Square Array

The representative sample for a material made up of solid cylinders in square array in a gas is shown in figure 2(c). The heat flow through the infinitesimal element of thickness dx is

$$dQ = \frac{k_s\, dx}{\sin\theta} (1 - t) \tag{6A}$$

or

$$dQ = \frac{k_g\, dx}{1 - \sin\theta} t \tag{7A}$$

Elimination of t from equations (6A) and (7A) and substitution of $x = \cos\theta$ and $dx = -\sin\theta\, d\theta$ result in

$$dQ = -\frac{k_g \sin\theta}{1 + \sin\theta\left(\frac{k_g}{k_s} - 1\right)} d\theta$$

Integration of this equation between the limits 0 and $\frac{\pi}{2}$ and replacement of Q by k result in

$$\frac{k}{k_g} = \frac{\pi}{2\left(\frac{k_g}{k_s} - 1\right)} - \frac{\frac{\pi}{2} - \sin^{-1}\left(\frac{k_g}{k_s} - 1\right)}{\left(\frac{k_g}{k_s} - 1\right)\sqrt{2\frac{k_g}{k_s} - \left(\frac{k_g}{k_s}\right)^2}}$$

which is the same as equation (2).

APPENDIX B

EXACT CALCULATION OF HEAT CONDUCTION THROUGH CYLINDERS BY RELAXATION METHOD

Calculations were made of the effective thermal conductivity of solid cylinders in gases for cylinders arranged in square array with the heat flow as shown in figure 2(a), for cylinders in square array with the heat flow at 45° to the direction shown in figure 2(a), and for cylinders in triangular array as shown in figure 2(d). In order to illustrate the relaxation method, the method is described for the calculation of heat flow through cylinders in square array with the heat flow as shown in figure 2(a). Calculations for the other cases are similar to these.

The heat flow through solid cylinders in square array in a gas can be determined by calculating the heat flow through the shape shown in figure 2(e). The temperature distribution must first be calculated. In order to apply the relaxation method, the material is replaced by a network of rods as shown in figure 2(e). The conductivity of the rods are proprotional to the medium (solid or gas) in which they are located. It is evident that the temperature distribution in the continuous materials is approximated by the temperature distribution in the rods and that the approximation becomes better as the distance between rods is decreased. For these calculations, the material was replaced by 11 vertical and 11 horizontal rods. For very high values of k_s/k_g, a finer grid was used in the vicinity of point c.

As a first step in the solution, the temperature at each of the intersections of the rods must be estimated. The heat flow into each of the intersections can be calculated. For an interior point such as point 1 (fig. 2(e)), the heat flow into the point is calculated from

$$Q_1 = \frac{k_{rs}}{\delta} A_r(t_3 - t_1) + \frac{k_{rs}}{\delta} A_r(t_2 - t_1) + \frac{k_{rs}}{\delta} A_r(t_5 - t_1) + \frac{k_{rs}}{\delta} A_r(t_4 - t_1)$$

$$= \frac{k_{rs}}{\delta} A_r(t_2 + t_3 + t_4 + t_5 - 4t_1)$$

or

$$\frac{Q_1\delta}{k_{rs}A_r} = R_1 = t_2 + t_3 + t_4 + t_5 - 4t_1 \tag{1B}$$

If the point were located in the interior of the gas instead of the solid, k_{rs} would be replaced by k_{rg} where $k_{rs}/k_{rg} = k_s/k_g$. The cross-sectional areas of the rods are all the same except for those located on the external boundarys where the areas are half as great because the rods replace half as much material as the internal rods. The surfaces ab and cd are insulated because of symmetry. For point 6,

$$Q_6 = \frac{k_{rs}}{\delta} A_r(t_8 - t_6) + \frac{k_{rs}}{\delta} \frac{A_r}{2} (t_9 - t_6) + \frac{k_{rs}}{\delta} \frac{A_r}{2} (t_7 - t_6)$$

or

$$R_6 = t_8 + \frac{t_9}{2} + \frac{t_7}{2} - 2t_6 \tag{2B}$$

For a point near the boundary between the solid and gas such as point 10,

$$Q_{10} = \frac{k_{rs}}{\delta} A_r(t_{13} - t_{10}) + \frac{k_{rs}}{\delta} A_r(t_{14} - t_{10}) +$$

$$\frac{k_{rs}}{\delta} A_r(t_{11} - t_{10}) + \frac{A_r}{\frac{l_1}{k_{rs}} + \frac{l_2}{k_{rg}}} (t_{12} - t_{10})$$

or

$$\frac{Q_{10}\delta}{k_{rs}A_r} \equiv R_{10} = t_{13} + t_{14} + t_{11} - 3t_{10} + \frac{1}{\frac{l_1}{\delta} + \frac{l_2}{\delta}\frac{k_{rs}}{k_{rg}}} (t_{12} - t_{10}) \tag{3B}$$

By use of equations similar to equations (1B), (2B), and (3B), the residual R is calculated for each intersection except for those on surfaces ad and bc, where the temperatures are known exactly. The values of R will, in general, be different from zero because of errors in the assumed temperature distribution. Each R is reduced to 0 by adjusting the temperature at the point. For example, if $R_1 = 0$ in equation (1B),

$$t_1 = \frac{t_2 + t_3 + t_4 + t_5}{4}$$

In this way a new temperature distribution is obtained which is closer to the correct distribution than the assumed one. The process is repeated until the temperature at each point does not change appreciably. In reducing the residuals to zero, it is customary to reduce the largest to zero first. For the present calculations, however, the process was usually found to converge faster when the residuals were reduced to zero in a certain pattern on the surface, for example, along diagonals.

With the temperature distribution calculated, the heat flow can be calculated from the temperature gradients at ad or bc. The agreement of the heat flows calculated at the two surfaces gives a check on the accuracy of the temperature distribution. The computed effective conductivities are estimated to be within 4 percent.

APPENDIX C

DERIVATION OF EQUATION FOR HEAT FLOW THROUGH CONCENTRIC CYLINDERS WITH VARIABLE THERMAL CONDUCTIVITY

The basic equation for heat conduction through a differential area dA is

$$dQ = - k \, dA \frac{dt}{dn} \tag{1C}$$

where n is the distance measured in the direction of heat flow. For concentric cylinders, the heat flow at a radius r is the same through all differential areas; so equation (1A) becomes, for concentric cylinders,

$$Q = - kA \frac{dt}{dr}$$

or

$$Q = - 2\pi r L k \frac{dt}{dr} \tag{2C}$$

Integration of equation (2C) between r and r_1 gives

$$Q \log_e \left(\frac{r}{r_1}\right) = 2\pi L \int_t^{t_1} k \, dt \tag{3C}$$

For most materials the variation of k with temperature can be represented with fair accuracy by an equation of the form

$$k = k_a + \alpha(t - t_a) \tag{4C}$$

where k_a is the conductivity at a reference temperature t_a and α is a constant. Substitution of equation (4C) into equation (3C) gives

$$Q \log_e \left(\frac{r}{r_1}\right) = - 2\pi L(t_1 - t) \left[k_a + \alpha\left(\frac{t_1 + t}{2} - t_a\right)\right] \tag{5C}$$

But from equation (4C) the expression in the bracket is k evaluated at $(t_1 + t)/2$. If k evaluated at $(t_1 + t)/2$ is written as k_m, equation (5C) becomes

$$Q = \frac{2\pi k_m L(t_1 - t)}{\log_e\left(\frac{r}{r_1}\right)}$$

which is the same as equation (3).

APPENDIX D

CORRECTION FOR SMALL ECCENTRICITY OF TUBES

In order to apply equation (3) it is necessary that the tubes be concentric. For nonconcentric tubes it is necessary to apply a correction to the position of the thermocouples in order to locate them at the position they would occupy if the tubes were concentric. For a given displacement of the center of the inner tube, it is desired to determine the displacement of a point between the tubes at a given temperature t. For small displacements of the inner tube along a radius, the temperature distribution along the radius is nearly the same as though the radius of the inner tube were increased by the amount of the displacement. (If the displacement is toward the center of the outer tube, the radius of the inner tube is decreased.) From equation (3)

$$t_1 - t = C \log_e \left(\frac{r}{r_1}\right) \tag{1D}$$

where the reference radius r_1 is taken as the radius of the outer tube. For $r = r_2$,

$$t_1 - t_2 = C \log_e \left(\frac{r_2}{r_1}\right) \tag{2D}$$

Elimination of C from equations (1D) and (2D) gives

$$t_1 - t = \frac{t_1 - t_2}{\log_e \left(\frac{r_2}{r_1}\right)} \log_e \left(\frac{r}{r_1}\right) \tag{3D}$$

If the radius of the inner tube is changed by an amount d, which is the displacement which must be applied to the inner tube along a particular radius in order to bring the center of the inner tube into line with the center of the outer tube, the radius where the temperature is t is changed from r to r' and C is changed to C', or

$$t_1 - t = C' \log_e \frac{r'}{r_1} \tag{4D}$$

and

$$t_1 - t_2 = C' \log_e \frac{r_2'}{r_1} \tag{5D}$$

where $r_2' = r_2 + d$ and the radii are measured from the center of the outer tube. From equations (4D) and (5D)

$$t_1 - t = \frac{t_1 - t_2}{\log_e\left(\frac{r_2'}{r_1}\right)} \log_e\left(\frac{r'}{r_1}\right) \tag{6D}$$

Elimination of $t_1 - t$ from equations (3D) and (6D) yields

$$\log_e\left(\frac{r'}{r_1}\right) = \frac{\log_e\left(\frac{r_2'}{r_1}\right)}{\log_e\left(\frac{r_2}{r_1}\right)} \log_e\left(\frac{r}{r_1}\right) \tag{7D}$$

The quantity r_2' must be determined for each set of thermocouples inasmuch as the displacement is different for different radial directions. The quantity r' is to be substituted for r in equation (4).

REFERENCES

1. Wilhelm, R. H., Johnson, W. C., Wynkoop, R., and Collier, D. W.: Reaction Rate, Heat Transfer, and Temperature Distribution in Fixed-Bed Catalytic Converters. Chem. Eng. Prog., vol. 44, no. 2, Feb. 1948, pp. 105-116.

2. Schumann, T. E. W., and Voss, V.: Heat Flow Through Granulated Material. Fuel in Science and Practice, vol. XIII, no. 8, Aug. 1934, pp. 249-256.

3. Eucken, A.: The Thermal Conductivity of Ceramic Refractory Materials. Its Calculation Based on the Thermal Conductivity of the Components. VDI Forschung. 353, March/April 1932. (Trans. by Gen. Elec. Co., July 11, 1950.)

4. Keyes, F. G.: Summary of Viscosity and Heat-Conduction Data for He, A, H_2, O_2, N_2, CO, CO_2, H_2O, and Air. Trans. A.S.M.E., vol. 73, no. 5, July 1951, pp. 589-596.

5. Tribus, Myron, and Boelter, L. M. K.: An Investigation of Aircraft Heaters. II - Properties of Gases. NACA ARR, Oct. 1942.

6. Lees, Charles H.: On the Conductivities of certain Heterogeneous Media for a Steady Flux having a Potential. Philosophical Magazine, vol. 49, 1900, pp. 221-226.

TABLE I - PARTICLE SIZE OF MAGNESIUM OXIDE.

Mesh	Sieve opening 12 S (in.)	Average percent MgO powder retained on sieve 100 f	Line number n
40	0.0166	None	1
60	.0098	33	2
80	.0070	22	3
100	.0059	10	4
140	.0041	10	5
170	.0035	8	6
200	.0029	3	7
325	.0017	8	8
Through 325	.0017	6	9

NACA

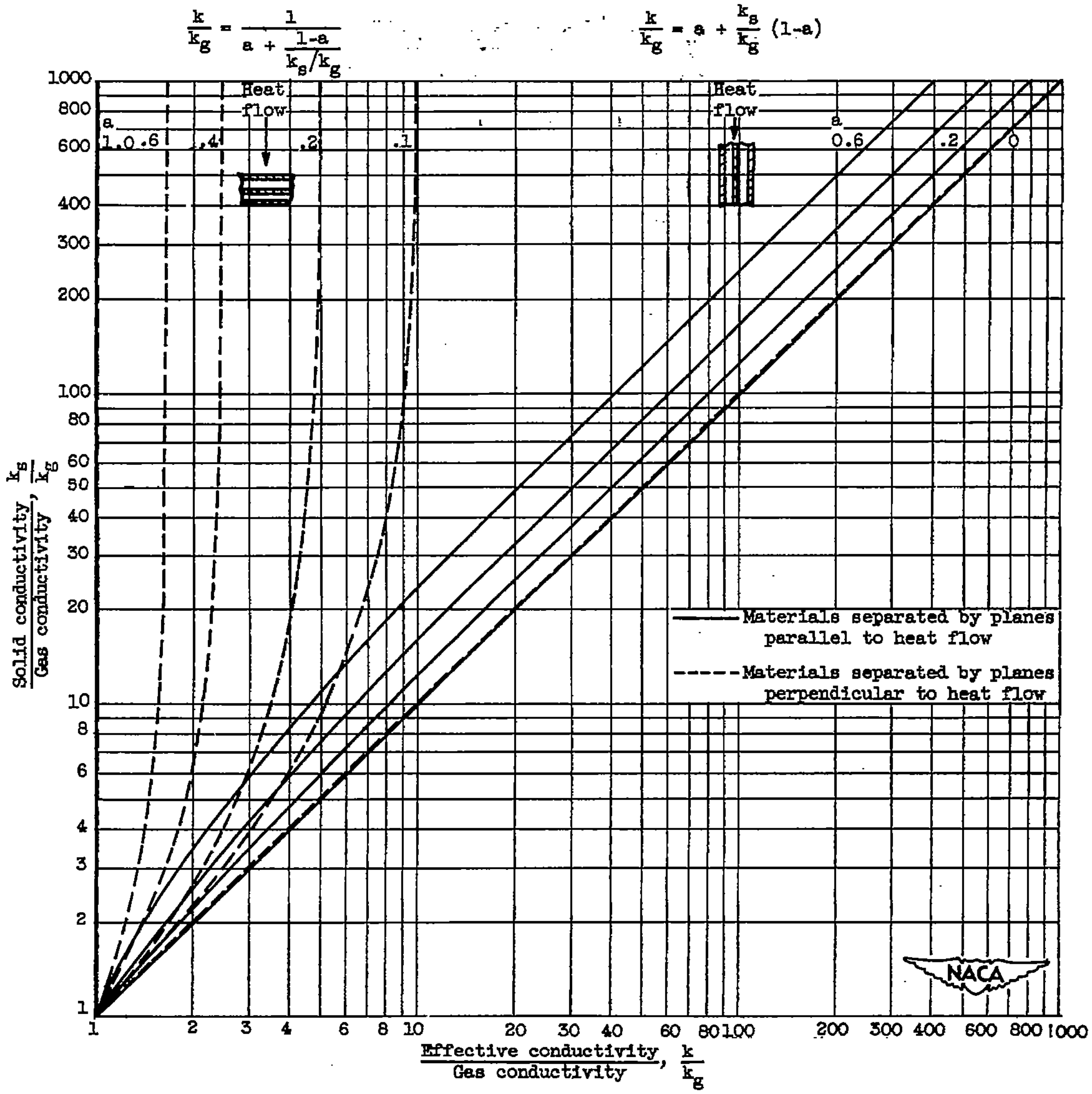

Figure 1. - Minimum and maximum effective thermal conductivities of two-phase systems; a, fraction of gas space.

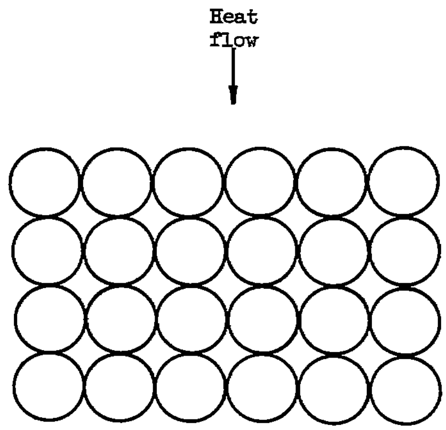

(a) Spheres or cylinders arranged in cubical or square array.

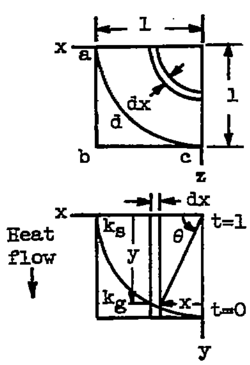

(b) Representative sample for spheres in cubical array.

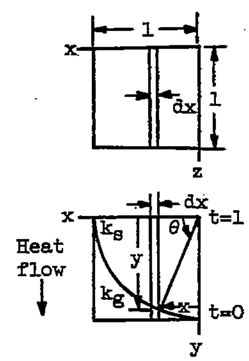

(c) Representative sample for cylinders in square array.

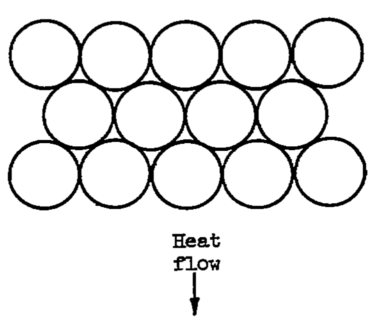

(d) Cylinders arranged in triangular array.

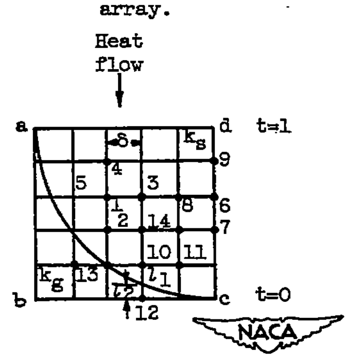

(e) Figure for calculating heat conducted through cylinders in square array by relaxation method.

Figure 2. - Figures used in analysis of thermal conductivities of powders.

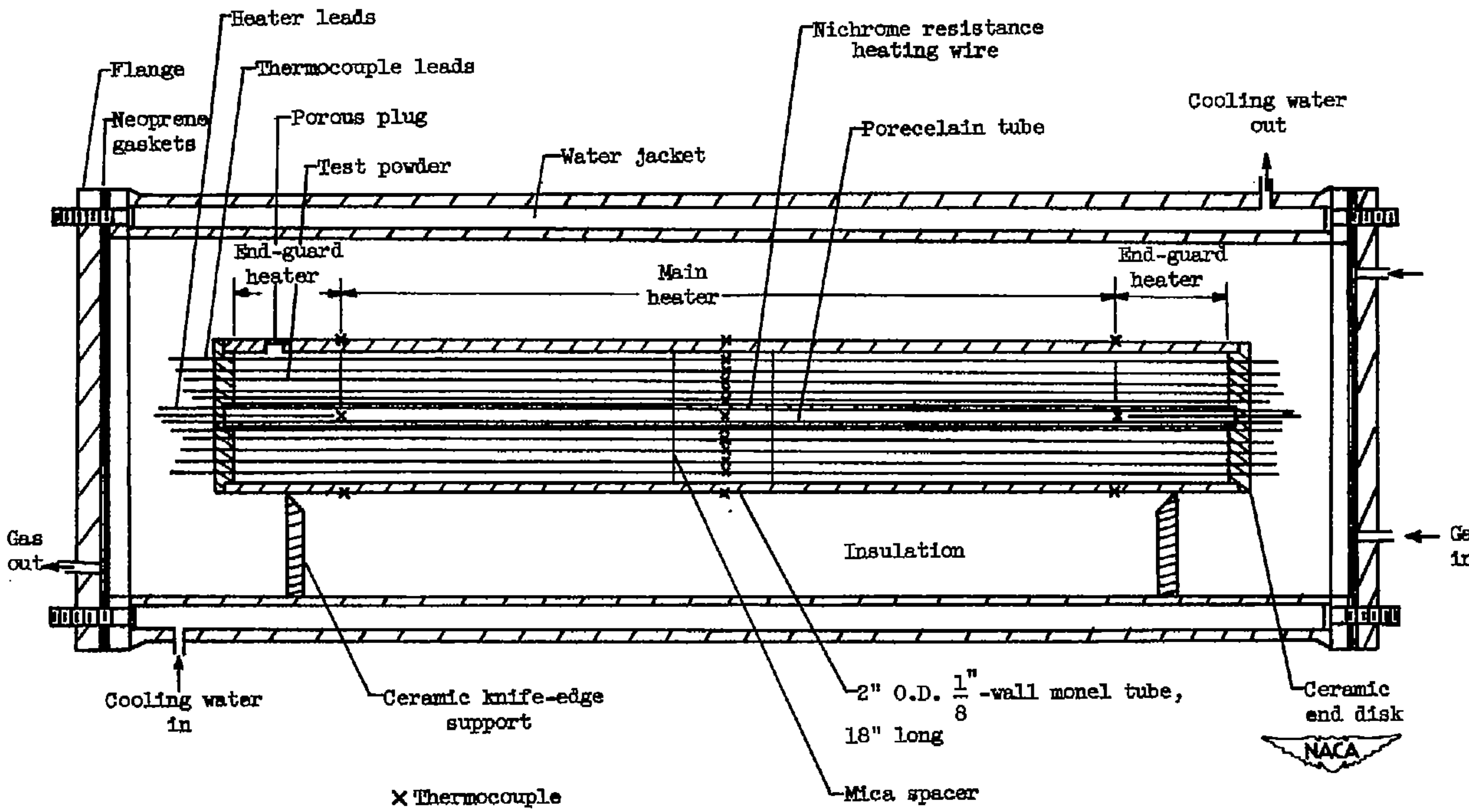

(a) Test section and gas chamber.

Figure 3. - Apparatus used for determination of thermal conductivities of powders in various gases.

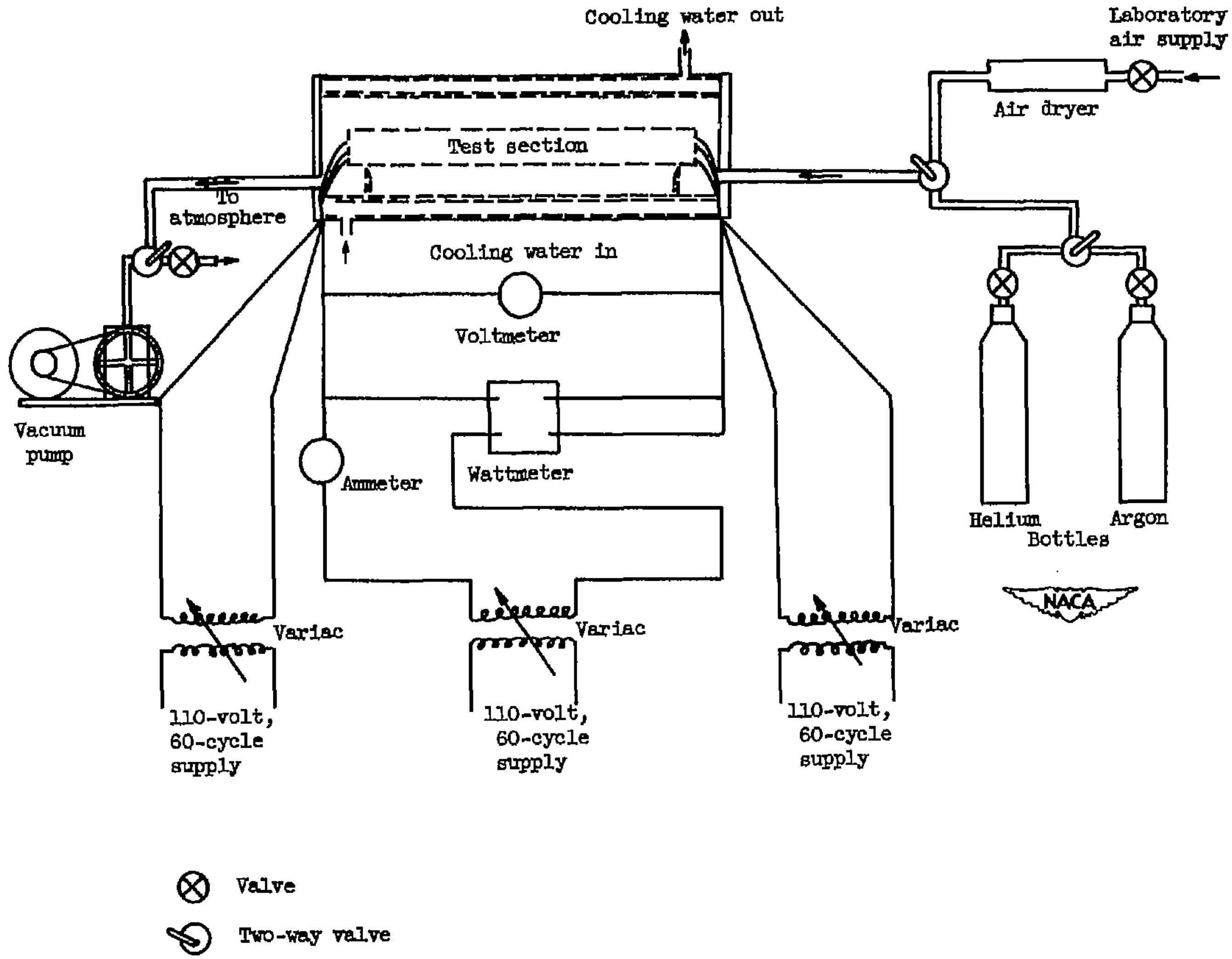

(b) Test section and associated equipment.

Figure 3. - Concluded. Apparatus used for determination of thermal conductivities of powders in various gases.

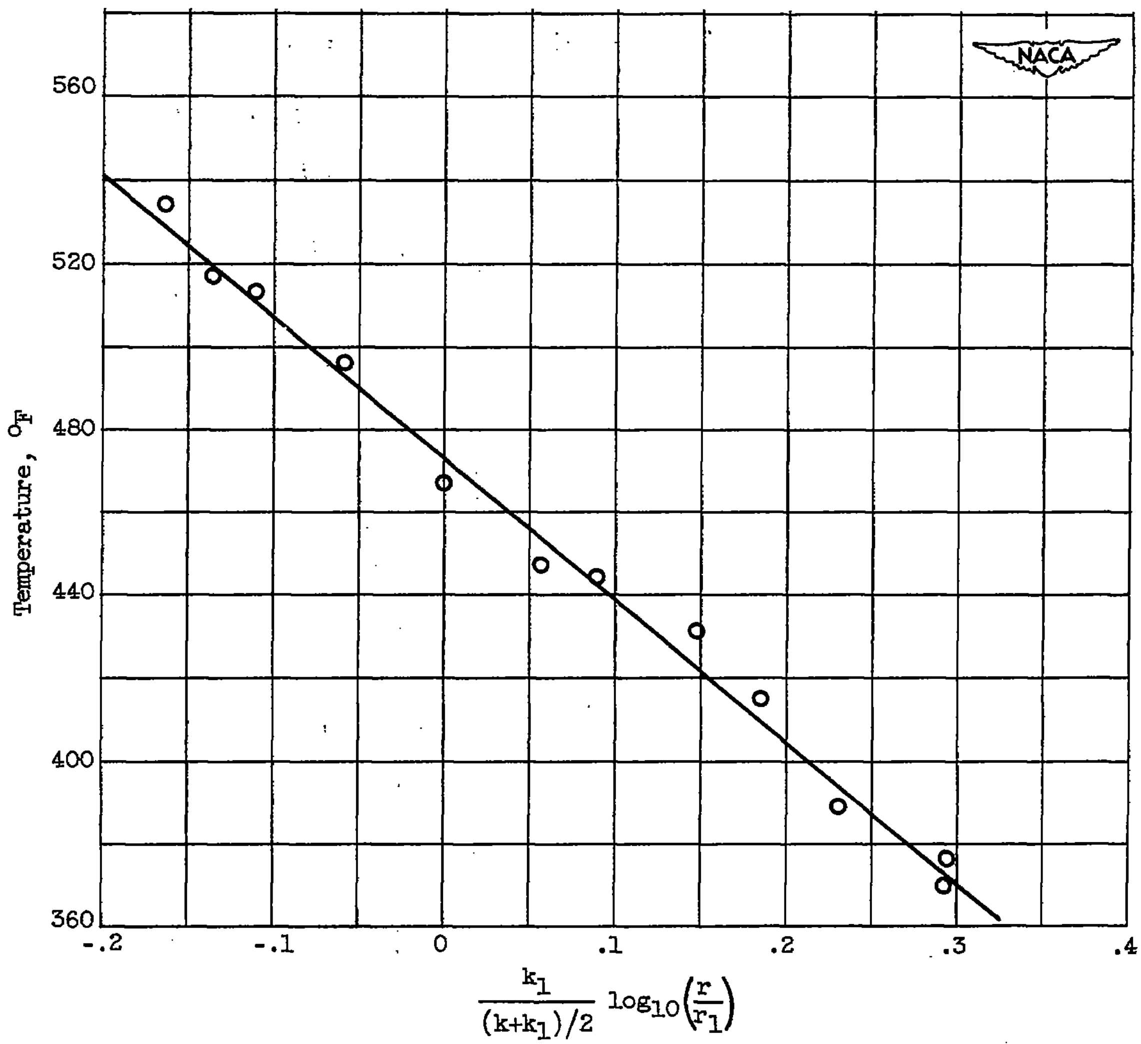

Figure 4. - Typical plot of radial temperature measurements for determination of thermal conductivity; k, effective conductivity; k_1, conductivity at r_1; r, radius; r_1, reference radius.

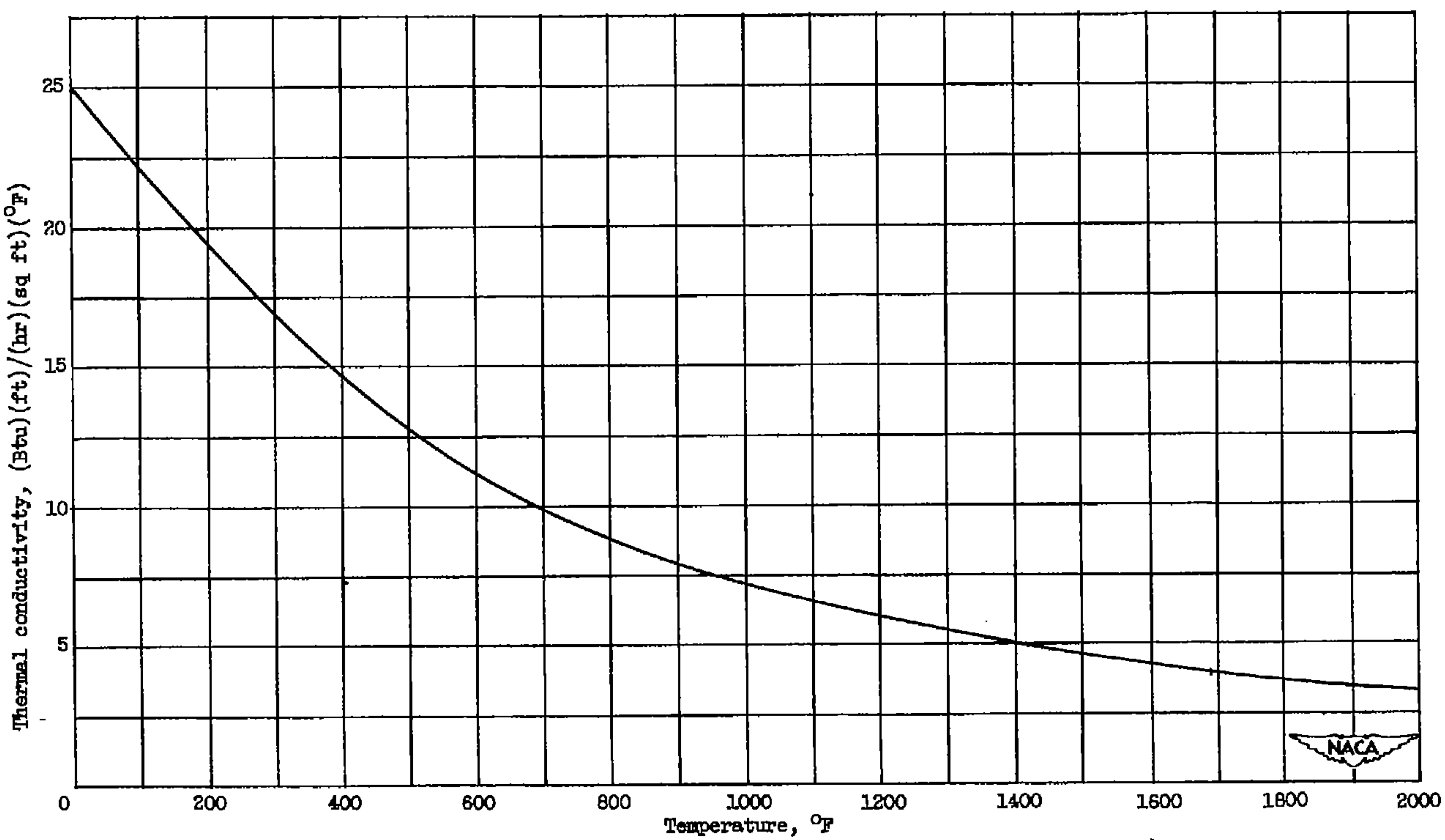

Figure 5. - Thermal conductivity of solid magnesium oxide from reference 3.

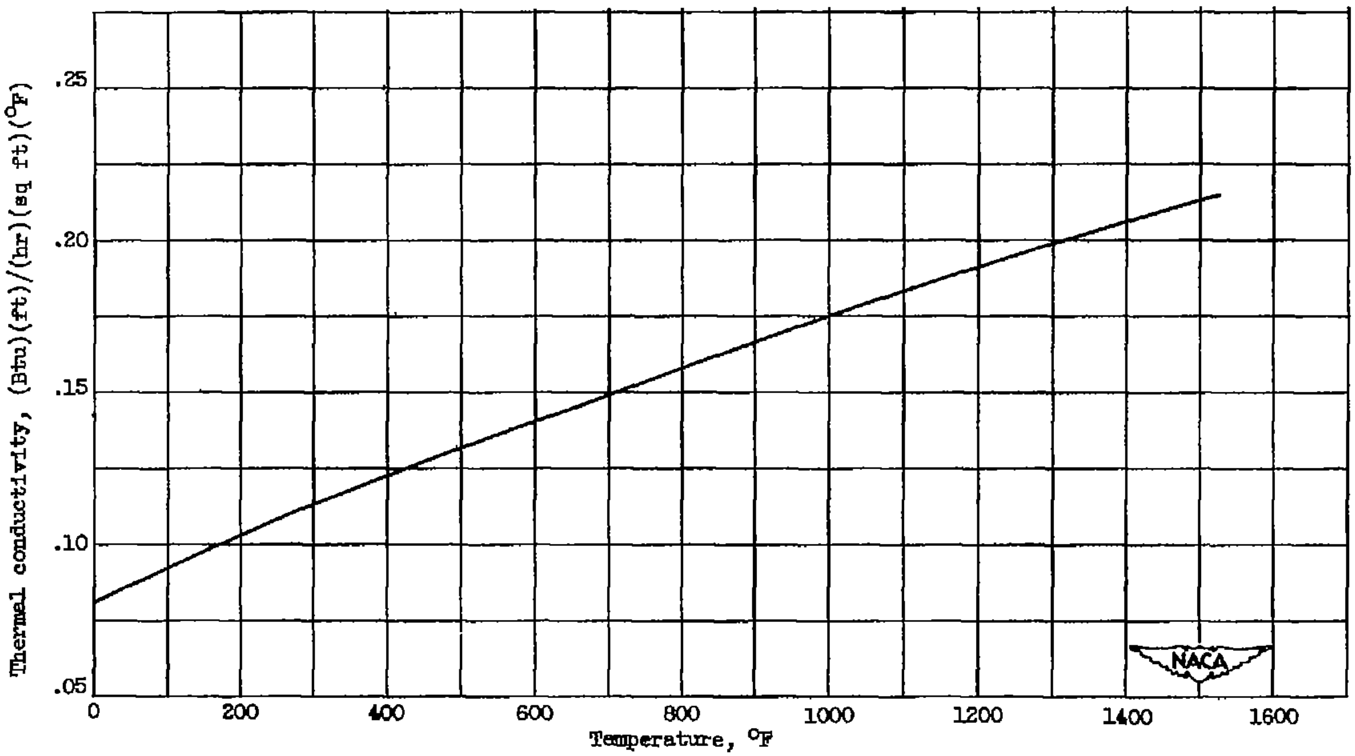

(a) Helium from kinetic theory.

Figure 6. - Thermal conductivities of gases.

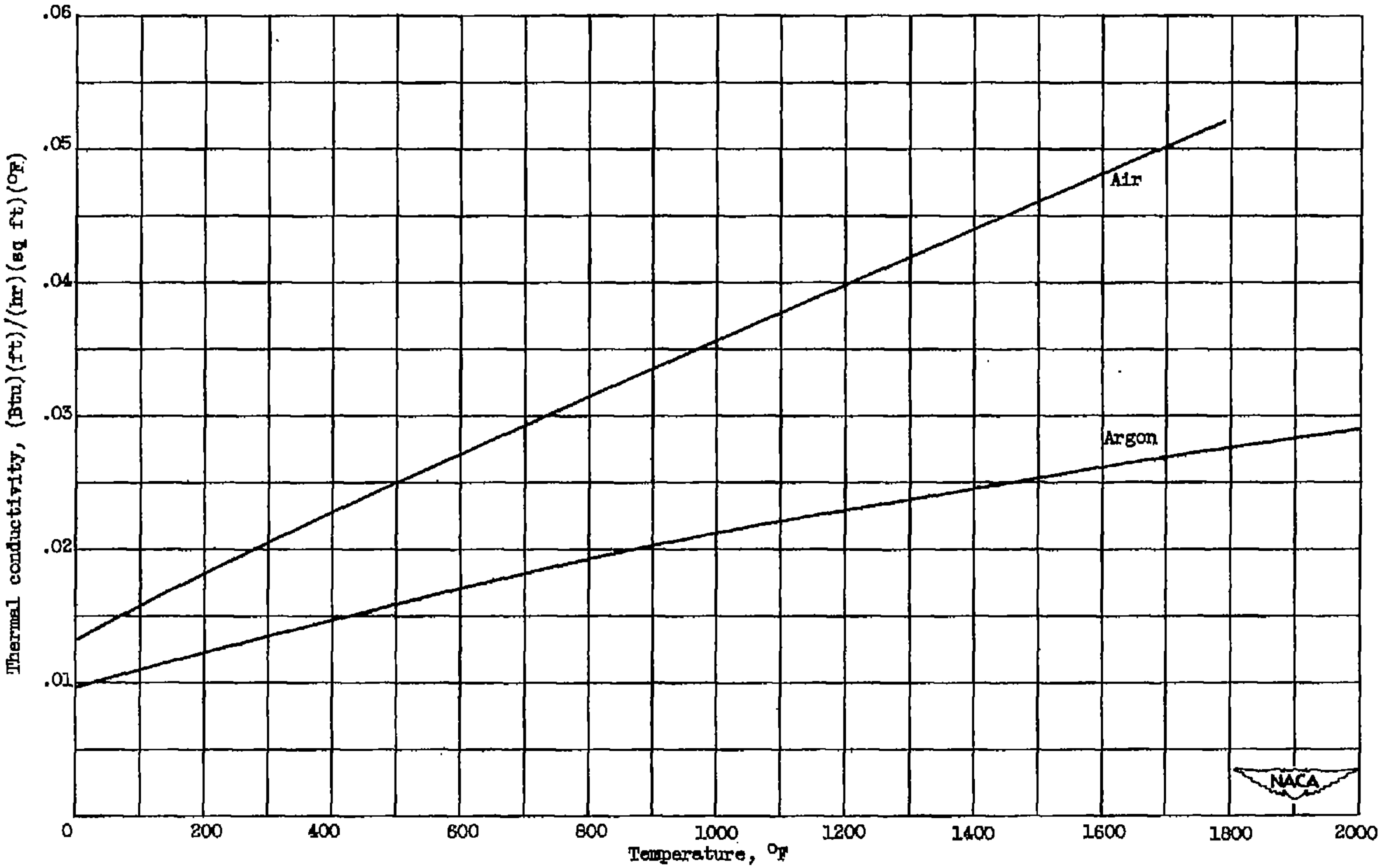

(b) Argon from kinetic theory and air from reference 5.

Figure 6. - Concluded. Thermal conductivities of gases.

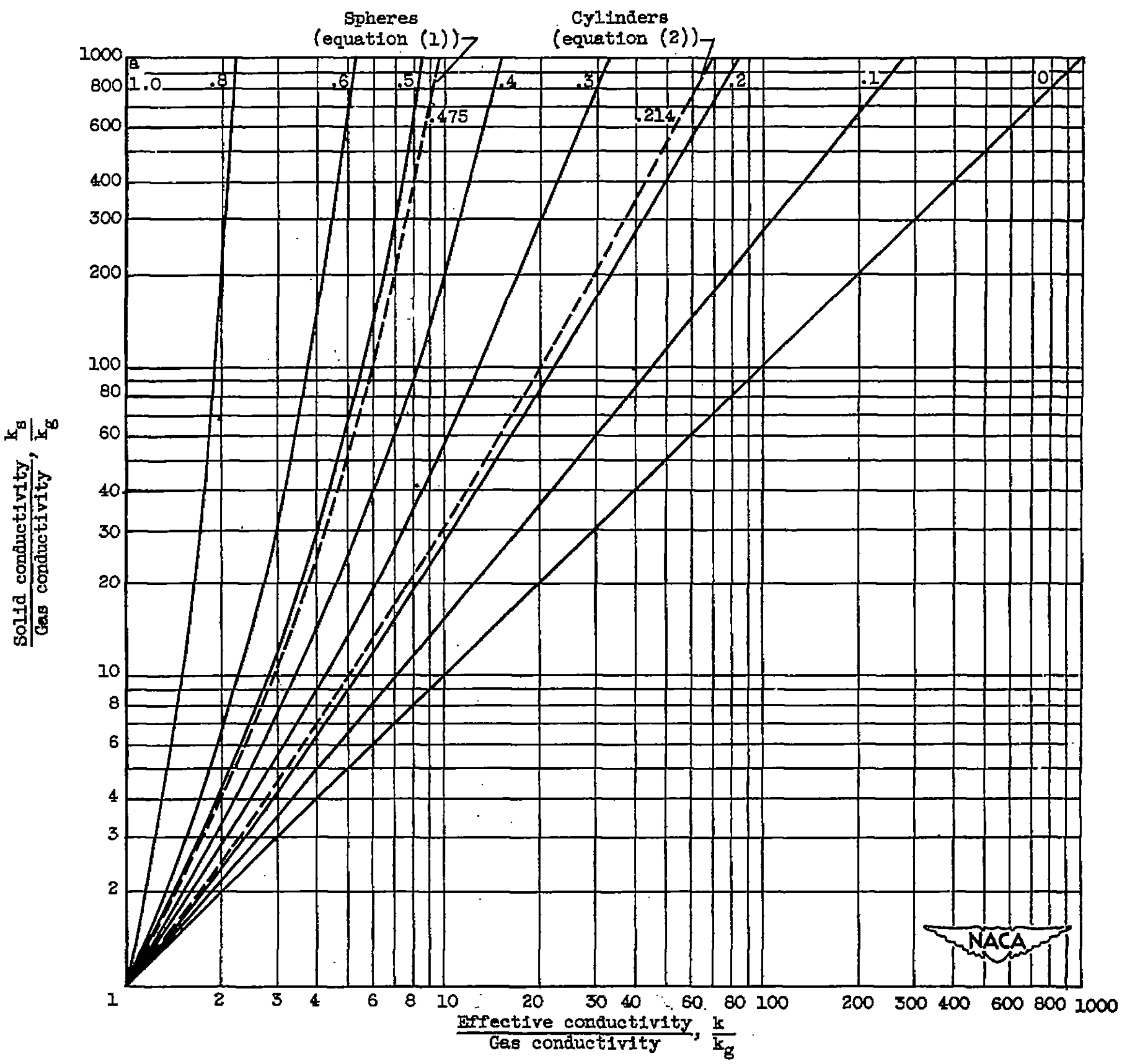

Figure 7. - Curves for predicting effective thermal conductivity of powder from simplified analysis; a, fraction of gas space.

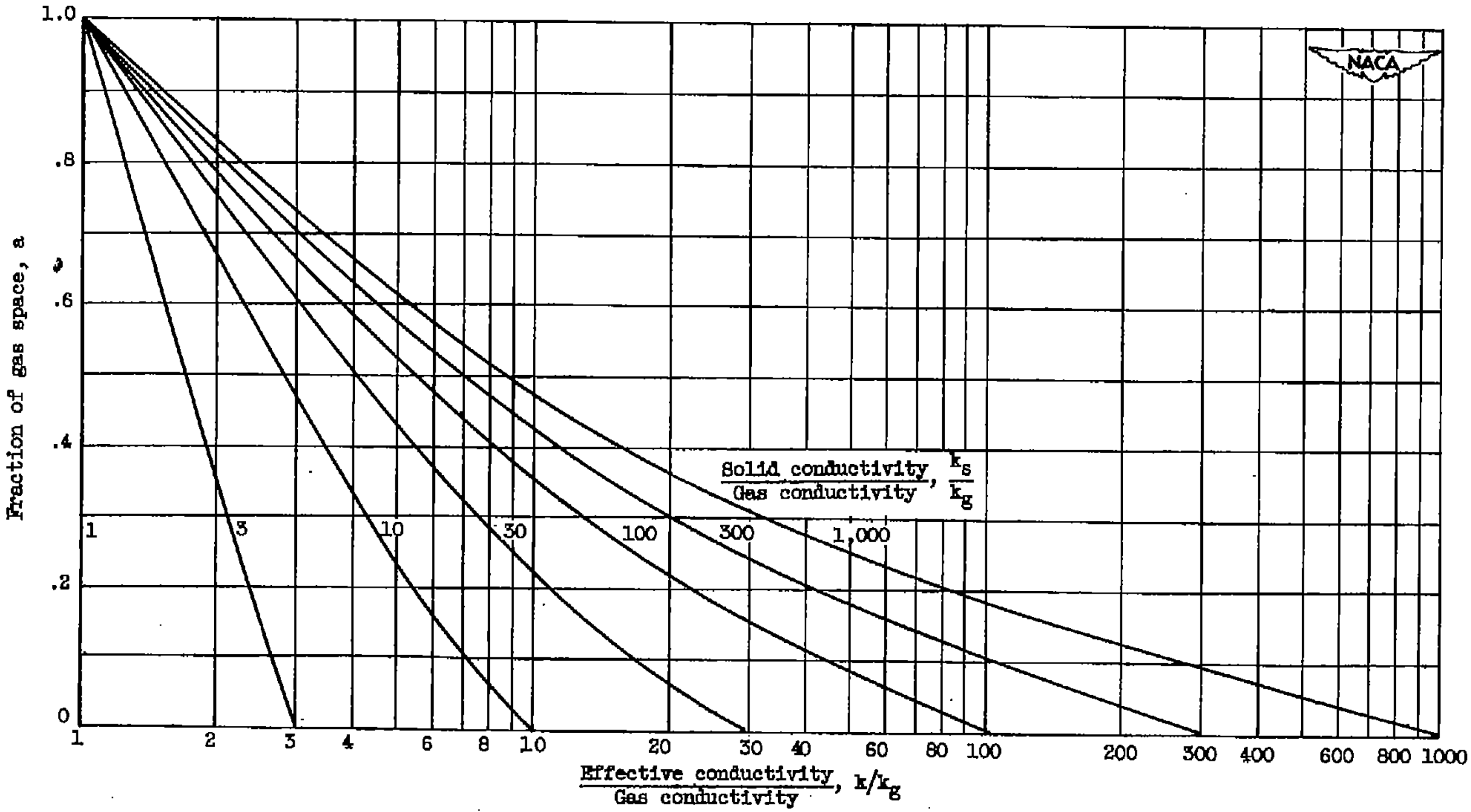

Figure 8. - Cross plot of figure 7.

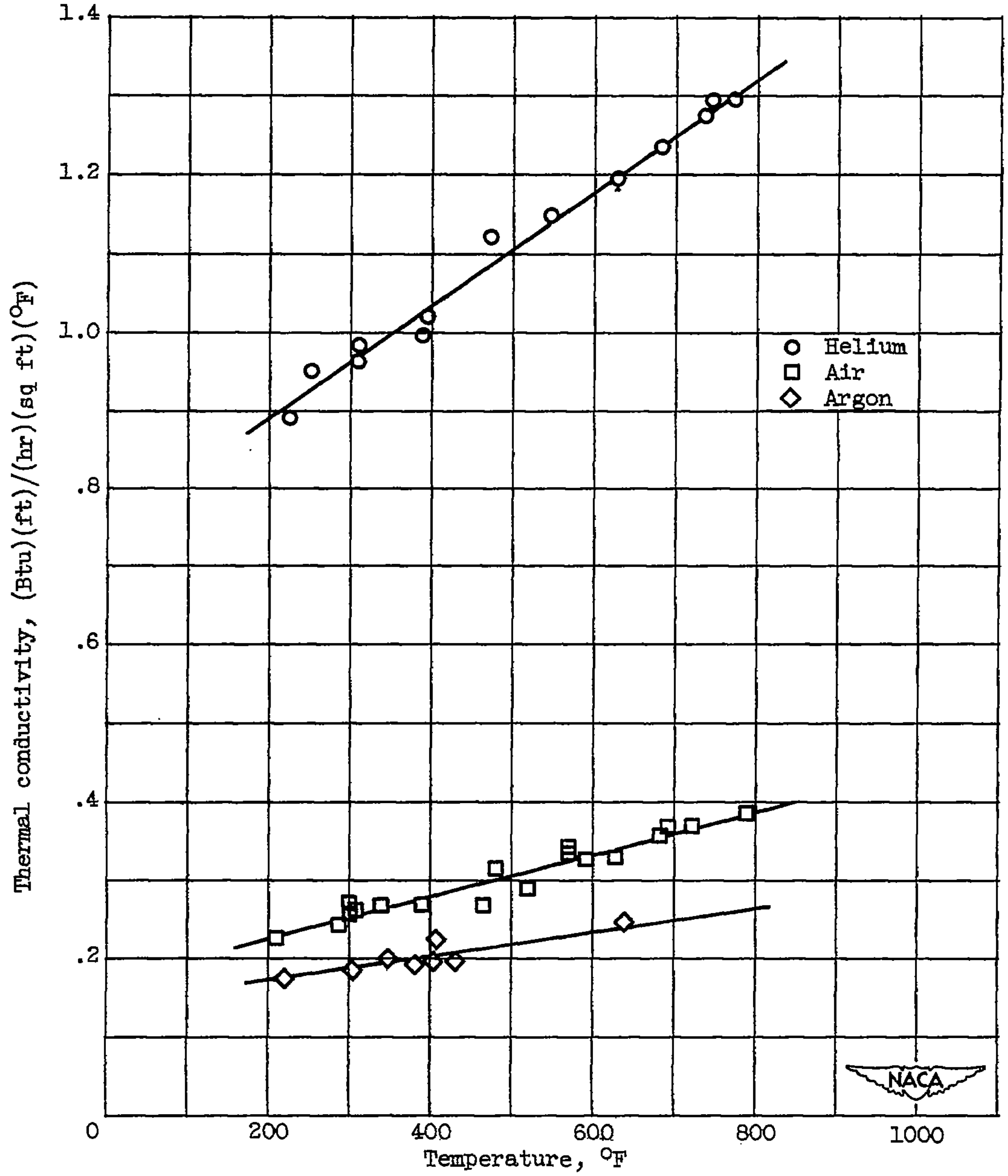

Figure 9. - Experimental thermal conductivities of magnesium oxide powder in various gases. Gas pressures in range where pressure change does not affect conductivity of powder.

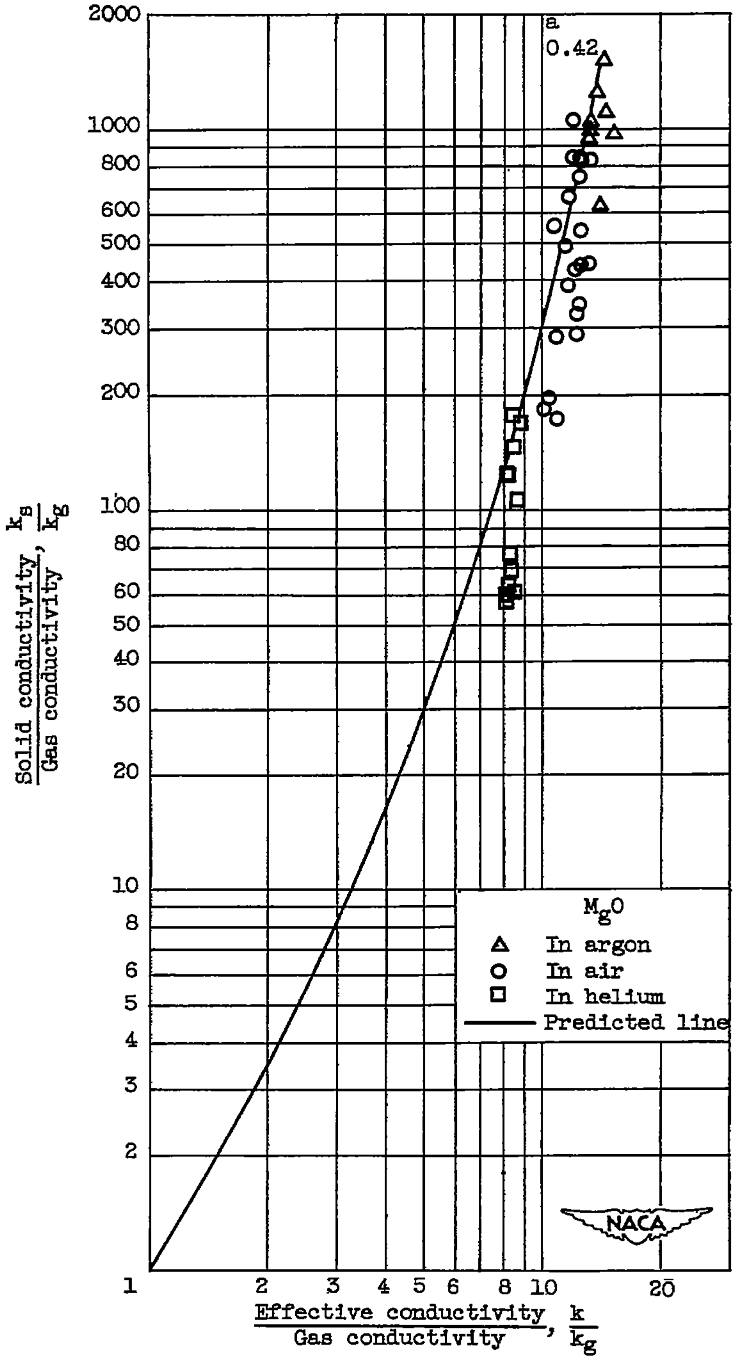

(a) Experimental results from present investigation.

Figure 10. - Comparison of analytical with experimental results. a, fraction of gas space.

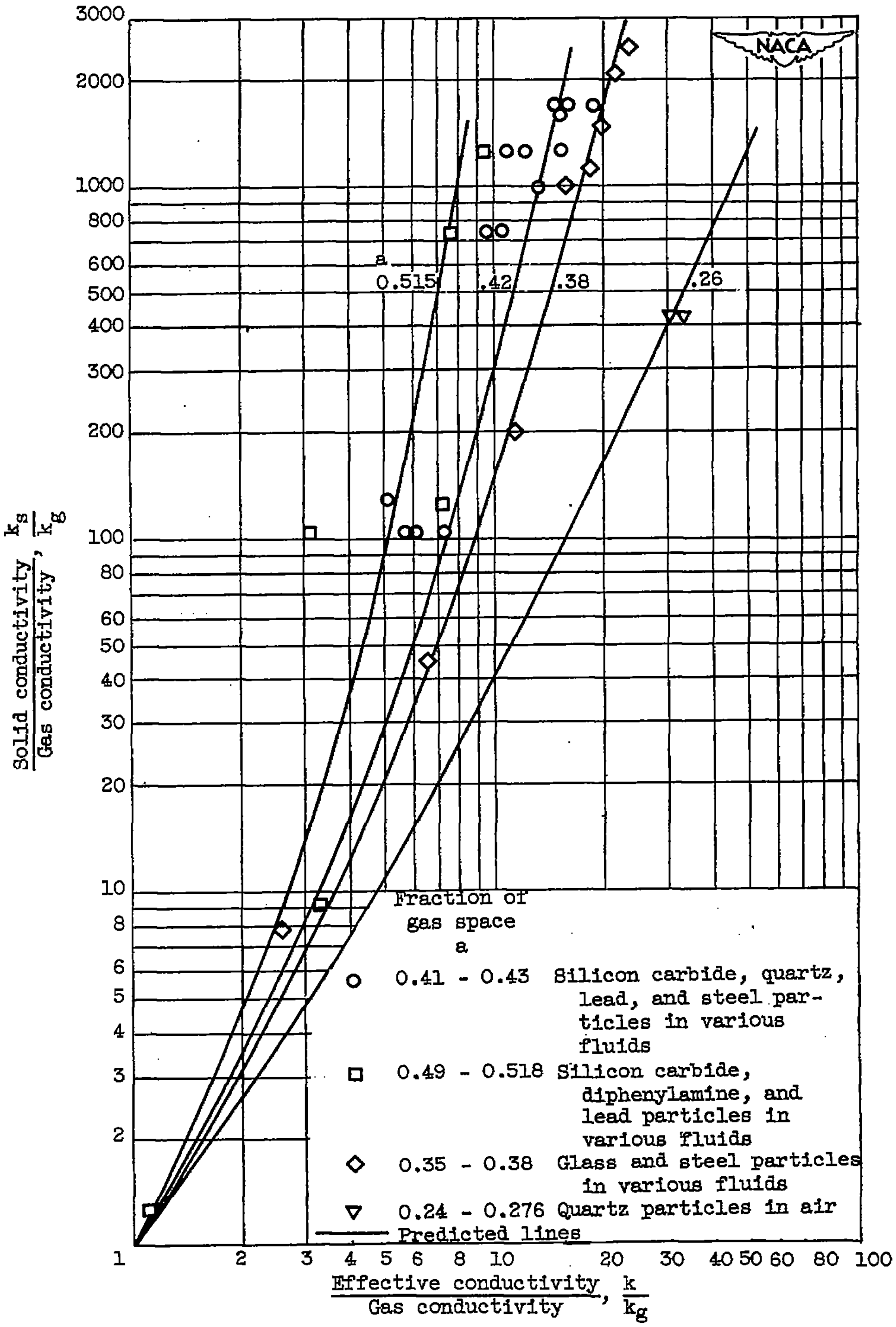

(b) Experimental results from other investigators (reference 1).

Figure 10. - Concluded. Comparison of analytical with experimental results. a, fraction of gas space.

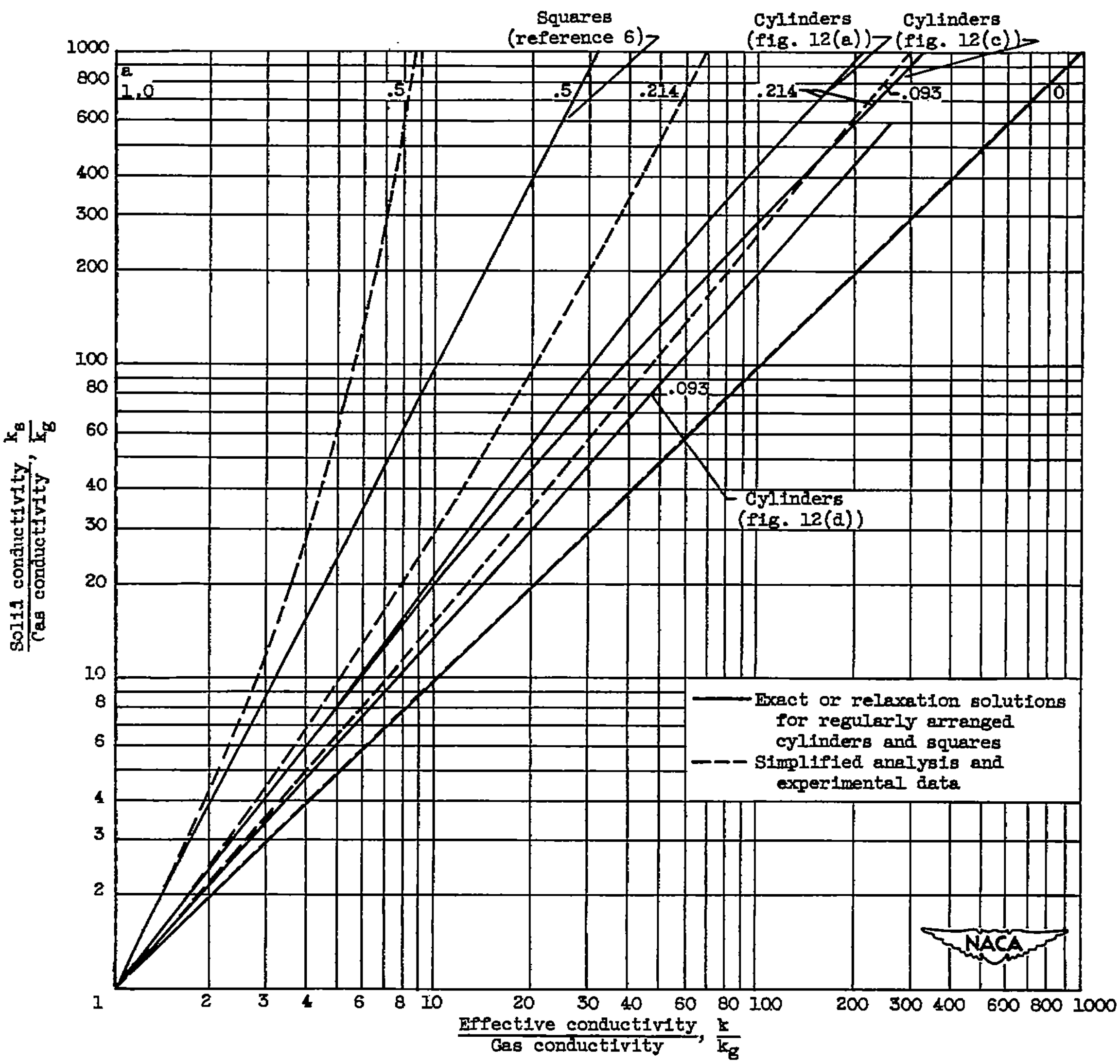

Figure 11. - Comparison of simplified analysis with exact or relaxation solutions showing effect of bending of heat-flow lines.

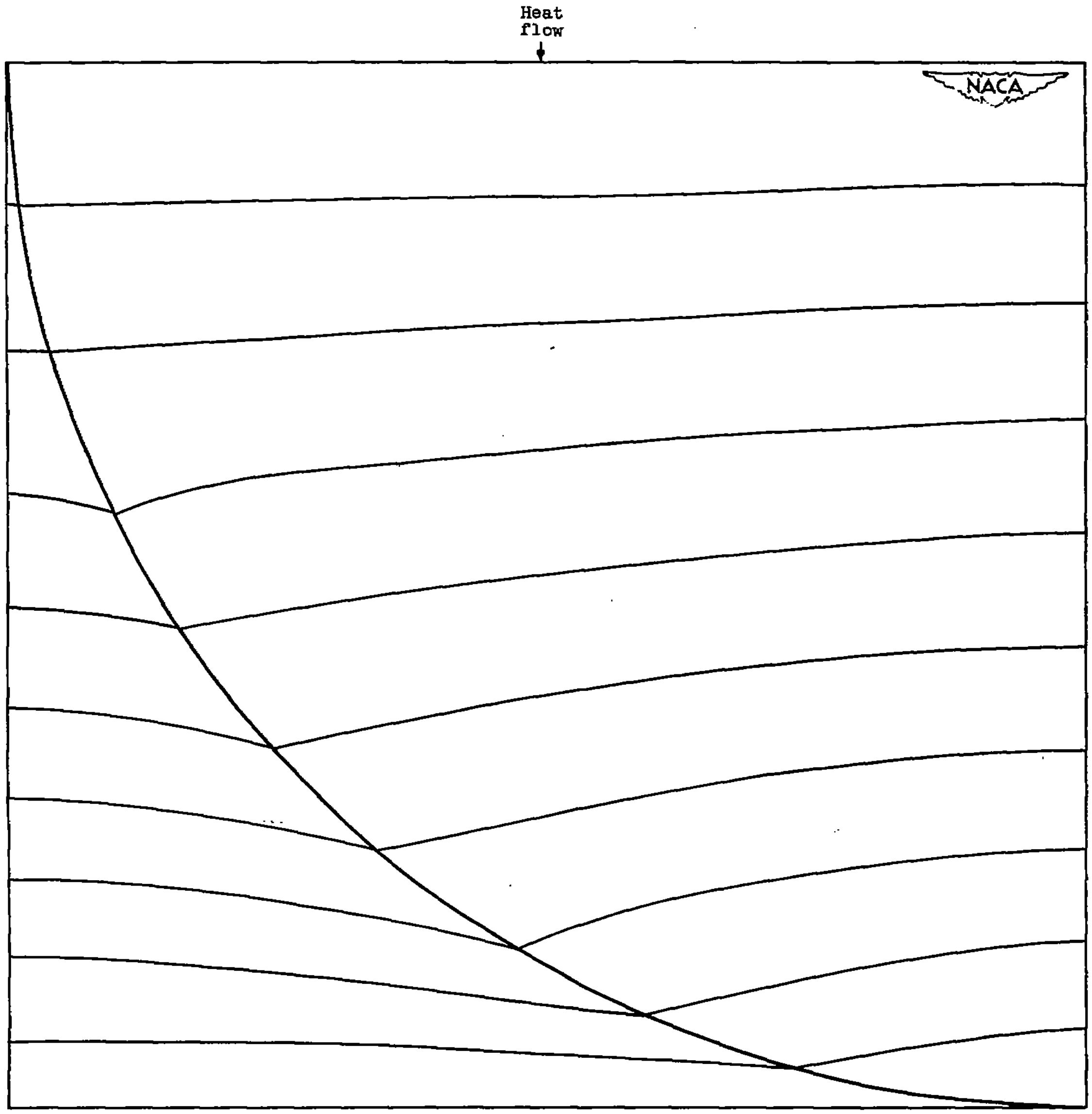

(a) In square array; ratio of solid conductivity to gas conductivity, 3.

Figure 12. - Constant temperature lines in representative sample of cylinders.

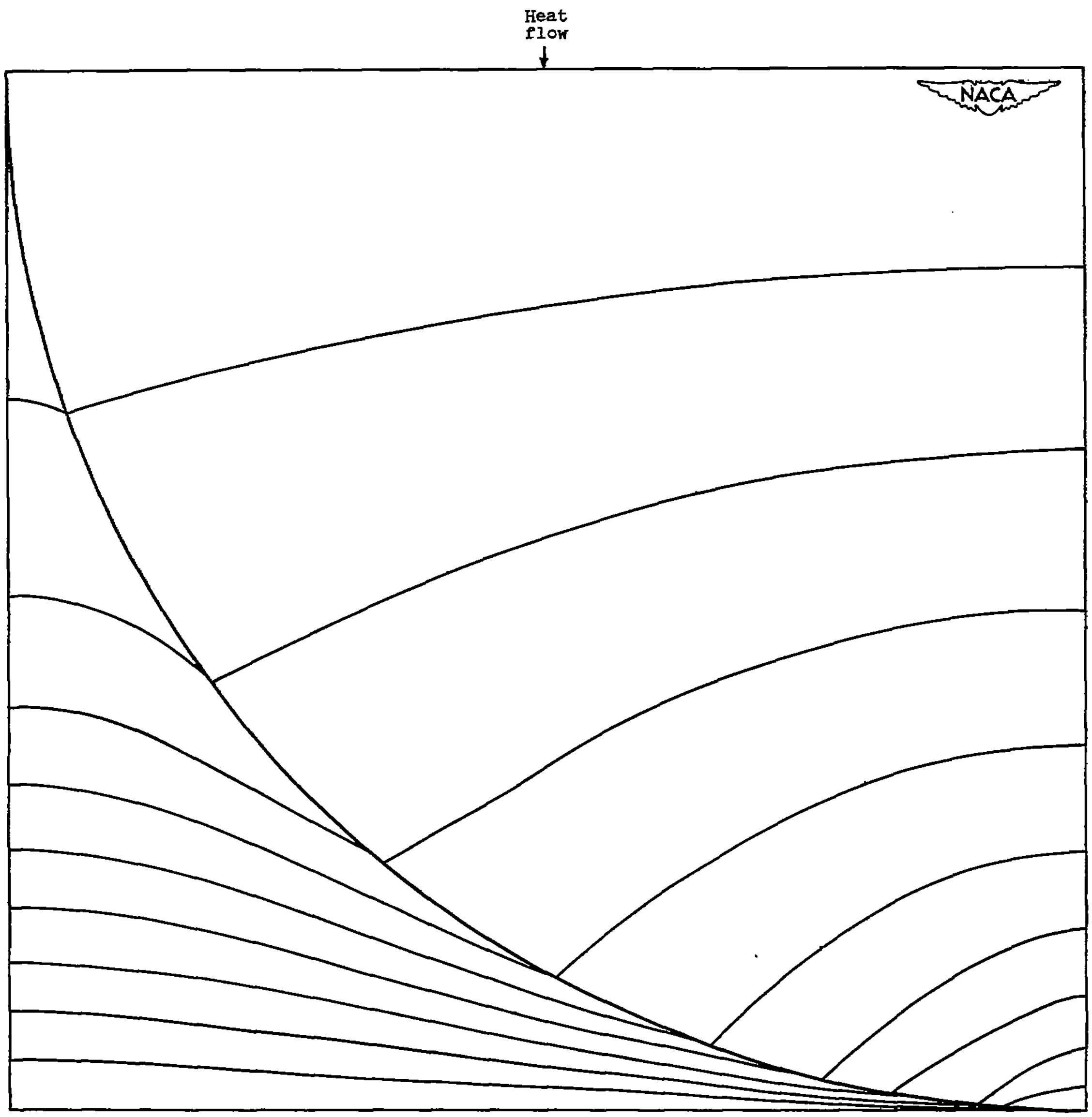

(b) In square array; ratio of solid conductivity to gas conductivity, 30.

Figure 12. - Continued. Constant temperature lines in representative sample of cylinders

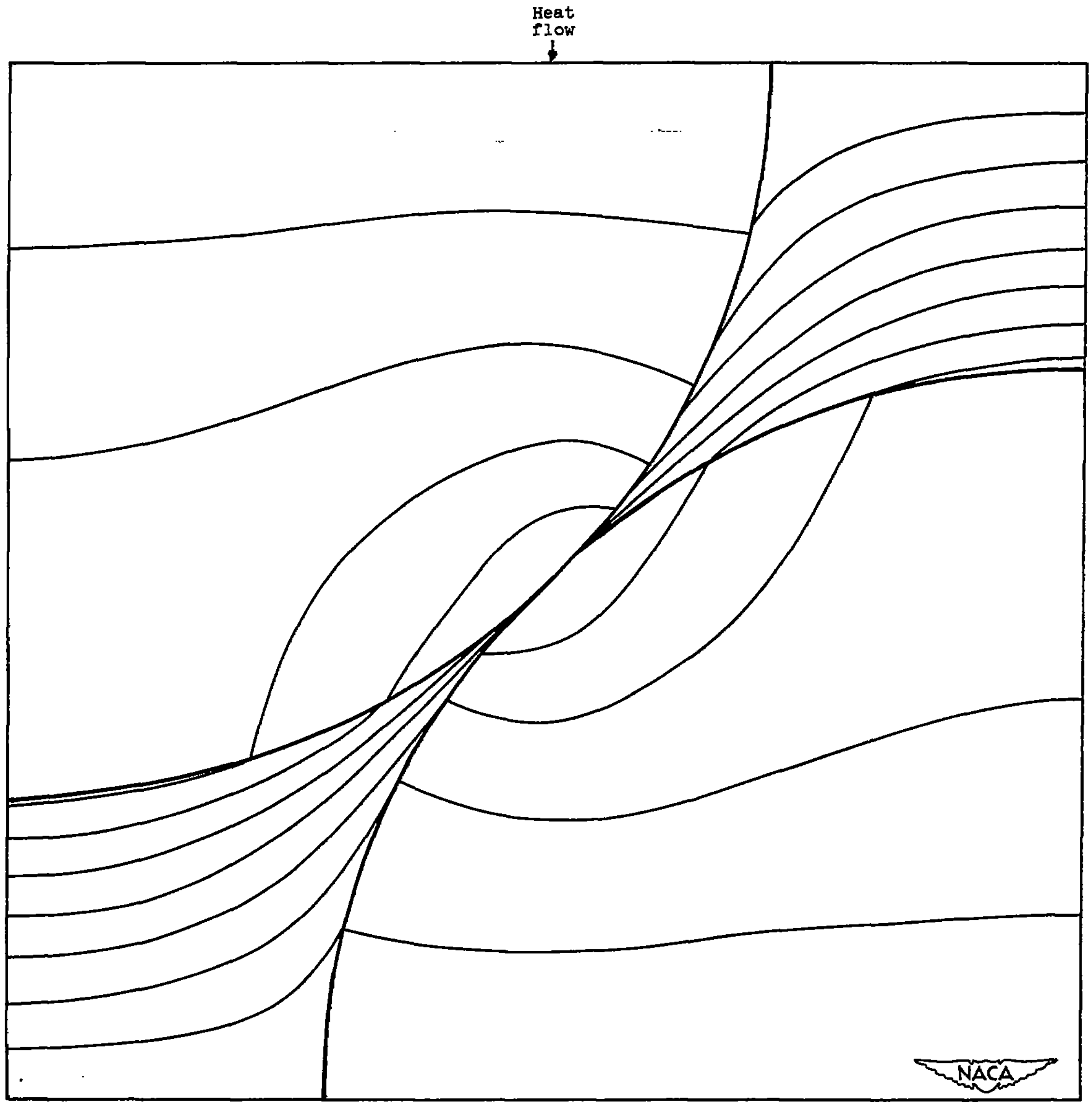

(c) In square array; ratio of solid conductivity to gas conductivity, 30; heat flow at 45° to heat flow in figures 12(a) and 12(b).

Figure 12. - Continued. Constant temperature lines in representative sample of cylinders.

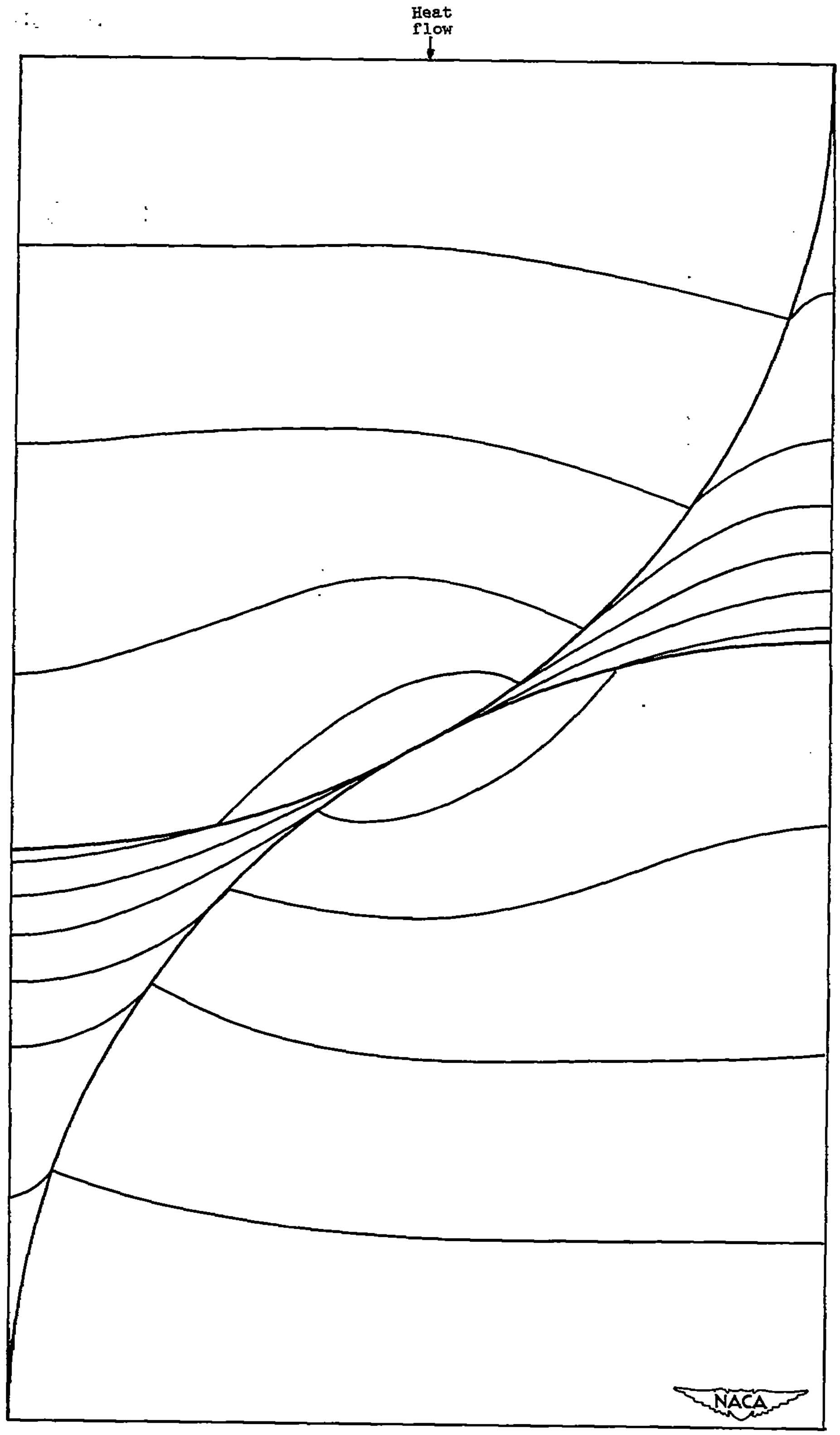

(d) In triangular array; ratio of solid conductivity to gas conductivity, 30.

Figure 12. - Concluded. Constant temperature lines in representative sample of cylinders.

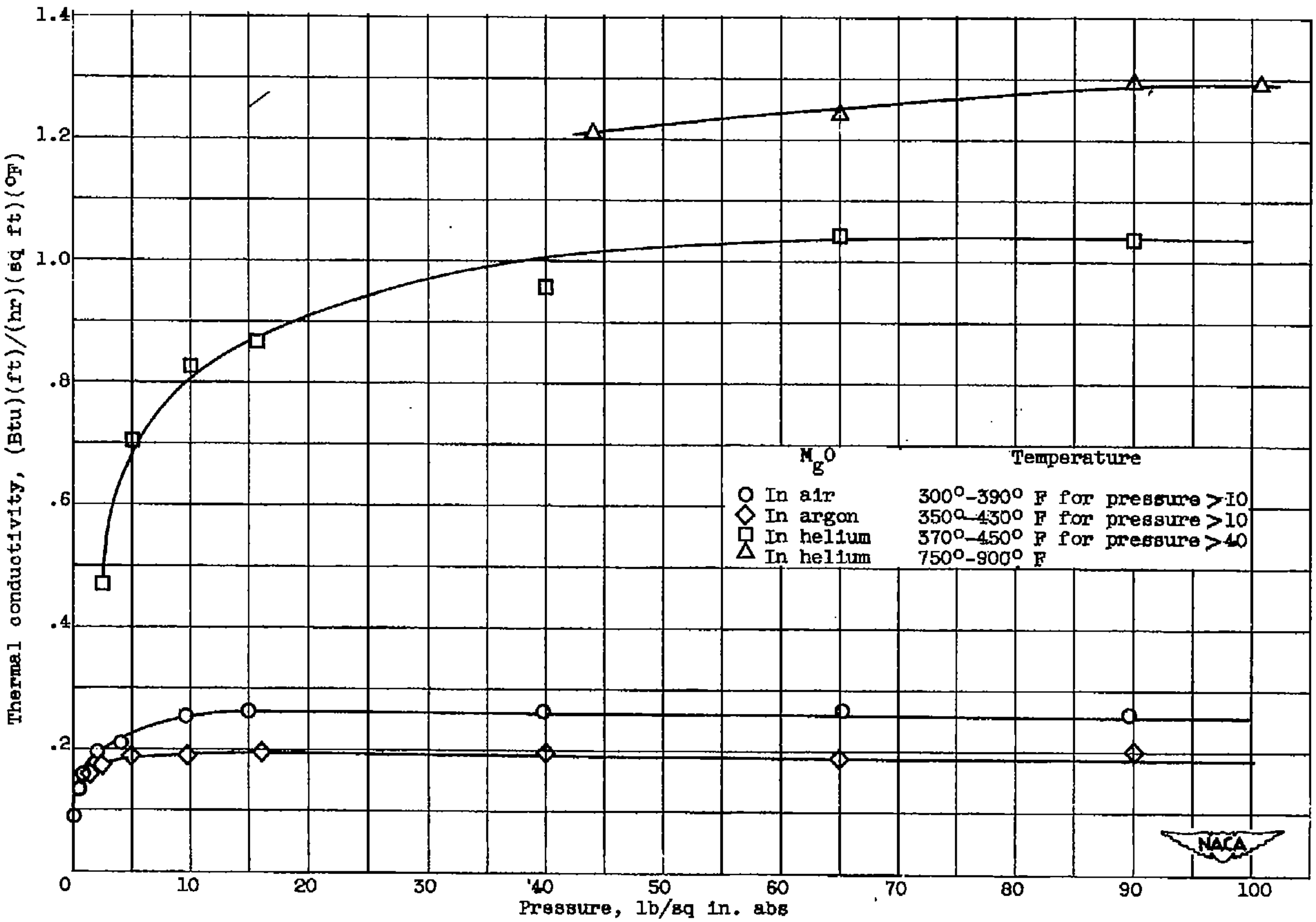

Figure 13. - Effect of gas pressure on thermal conductivity of magnesium oxide powder in various gases.